Available online at www.sciencedirect.com
ScienceDirect
Mathematics and Computers in Simulation 216 (2024) 145–167
MATHEMATICS AND COMPUTERS IN SIMULATION
www.elsevier.com/locate/matcom

Original articles

Stokes problem with the Coulomb stick–slip boundary conditions in 3D: Formulations, approximation, algorithms, and experiments

Jaroslav Haslinger[a,b], Radek Kučera[a,b], Kristina Motyčková[b,*], Václav Šátek[c,b]

[a] *Faculty of Mechanical Engineering, VŠB-TUO, 17. listopadu 2172/15, 708 00 Ostrava-Poruba, Czech Republic*
[b] *IT4Innovations, VŠB-TUO, 17. listopadu 2172/15, 708 00 Ostrava-Poruba, Czech Republic*
[c] *Faculty of information technology, Brno University of Technology, Božetěchova 1/2, 612 66 Brno, Czech Republic*

Received 16 May 2023; received in revised form 11 August 2023; accepted 23 August 2023
Available online 28 August 2023

Abstract

The paper deals with the approximation and numerical realization of the Stokes system in 3D with Coulomb's slip boundary conditions. The weak velocity–pressure formulation leads to an implicit inequality type problem which is discretized by the P1+bubble/P1 elements. To regularize the discrete non-smooth slip term and to release the discrete impermeability condition the duality approach is used. For numerical realization of the resulting saddle-point problem two strategies are proposed, namely (i) its fixed-point formulation solved by the method of successive approximations (ii) the direct numerical solution of the saddle-point problem. The semi-smooth Newton method is used to solve non-smooth equations appearing in both these approaches.

Keywords: Stokes problem; Coulomb stick–slip boundary conditions; Successive approximations; Semi-smooth Newton method

1. Introduction

The no-slip boundary condition, i.e. the velocity vector $\boldsymbol{u} = \boldsymbol{0}$ on the solid surface is a standard one in fluid flow models. It characterizes the adhesion of a liquid to the surface. However there are situations, depending on characteristics of a liquid (polymers, e.g) or walls (surfaces coated by hydrophobic materials) when a certain slip is observed. The first slip condition was formulated by Navier who postulated that the tangential component $\boldsymbol{u}_\tau$ of $\boldsymbol{u}$ which represents the slip velocity is a linear function of the shear stress $\boldsymbol{\sigma}_\tau$. Later on this law has been extended to more sophisticated nonlinear relations but still formulated by single-valued functions. A justification of different slip boundary conditions from the physical point of view is done in [31] and the references therein.

From the Navier slip condition we see that a slip occurs whenever $\boldsymbol{\sigma}_\tau \neq \boldsymbol{0}$ at the wall, i.e. the response is immediate. But this is not true, in general. Consider for example a water drop on an inclined plane whose surface

* Corresponding author.
E-mail address: kristina.motyckova@vsb.cz (K. Motyčková).

https://doi.org/10.1016/j.matcom.2023.08.036

is coated by a teflon film. The drop starts sliding only if the angle of inclination attains certain critical value. Below this value the drop still adheres to the wall.

A large class of such stick–slip boundary conditions can be written as follows:

$$\begin{aligned} |\boldsymbol{\sigma}_\tau| &\leq g, \\ \text{if } \boldsymbol{u}_\tau \neq \mathbf{0} \text{ then } \boldsymbol{u}_\tau \cdot \boldsymbol{\sigma}_\tau &= -g|\boldsymbol{u}_\tau|, \end{aligned} \tag{1.1}$$

where g stands for a threshold stick–slip bound and $|\cdot|$ is the magnitude of a physical quantity (the absolute value or the Euclidean norm depending on the spatial dimension). This condition is completed with the impermeability condition $u_\nu = 0$. The second condition in (1.1) says that a slip occurs only if $|\boldsymbol{\sigma}_\tau| = g$. On the other hand, if $\boldsymbol{u}_\tau = \mathbf{0}$, then $|\boldsymbol{\sigma}_\tau|$ belongs to the interval $\langle -g, g\rangle$. Thus the constitutive law between $\boldsymbol{\sigma}_\tau$ and $\boldsymbol{u}_\tau$ is now given by a multi-valued mapping usually represented by the subgradient of an appropriate, generally nonsmooth convex slip functional j [34]. Let us emphasize that the partition of the surface into the sticking/slipping part is one of unknowns of the problem. We meet the same type of boundary conditions in frictional contact solid mechanics.

Weak formulations of mathematical models involving the stick–slip conditions (1.1) lead to inequality type problems for $\boldsymbol{u}$ and the pressure p just because of the presence of j. Their complexity depends on the definition of g in (1.1). If g is known a-priori (corresponding to the Tresca model of friction in contact mechanics), the mathematical model is given by an inequality type problem of the second kind using the terminology in [18]. Its mathematical analysis has been done by Fujita in [15,16]. The case when g depends on the slip velocity magnitude, i.e. $g := g(|\boldsymbol{u}_\tau|)$ is more involved from the mathematical point of view since the slip functional j depends on the solution itself. This model has been theoretically studied in [32,33] for the Stokes and Navier–Stokes equations. Finally there is an important class of slip laws with g depending on the magnitude of the normal stress σ_ν. This paper is devoted to one of them, namely to local Coulomb's type slip conditions mentioned in [31]. In this case $g = \mathscr{F}|\sigma_\nu|$, where $\mathscr{F}$ is a slip coefficient. The corresponding mathematical model leads again to an implicit inequality type problem as j depends on the unknown σ_ν. But this time the whole matter is much more complicated compared with the previous one owing to the character of σ_ν. Without additional assumptions on the solution, the normal stress is no longer represented by a function. It has to be interpreted as a functional defined on the trace space of kinematically admissible functions. This lack of regularity makes impossible to define $|\sigma_\nu|$. One way to overcome this fundamental difficulty is to change the slip model. For instance, to replace local Coulomb's slip law by its non-local version which uses a regularized form of σ_ν [6,10]. Another way to make the definition of g meaningful is to establish some regularity results. Saito proved in [34] that if the boundary $\partial\Omega$ consists of two sufficiently smooth connected components Γ_D and Γ, such that $dist(\Gamma_D, \Gamma) > 0$, with the Dirichlet, and Tresca type slip conditions, respectively, then the solution $(\boldsymbol{u}, p)$ to the Stokes system belongs to $(H^2(\Omega))^d \times H^1(\Omega)$ provided that $g \in H^{1/2}(\Gamma)$. This could be a way, together with a fixed-point approach, to prove the existence of a solution to the problem with local Coulomb's slip conditions. As a matter of interest, this basic difficulty concerning the definition of g does not exist in contact problems for solids with Coulomb's friction. In this case the set of kinematically admissible displacements is convex and it consists of functions satisfying unilateral boundary conditions. The normal stress σ_ν can be interpreted as the Lagrange multiplier releasing these unilateral constraints and becomes now a signed quantity. Therefore the absolute value of σ_ν in the definition of g disappears.

Numerical analysis (theory and also an implementation) of this class of problems is relatively a new area. It combines techniques of computational fluid mechanics for incompressible fluids [17] and numerical analysis for variational inequalities [18]. Approximations are based on finite element discretizations of alternative variants of the weak velocity–pressure formulation. Since the slip functional j which appears in the weak formulation is nondifferentiable, in general, it is convenient to regularize it just from computational purposes. One of possible ways how to do that is to use a duality approach. Its advantage is that the resulting Lagrange multiplier can be interpreted as the shear stress $\boldsymbol{\sigma}_\tau$. For the error and convergence analysis as well as computational techniques for the Stokes and Navier–Stokes equations with different types of threshold slip boundary conditions we refer to [4,5,11,12,21,22,25].

The main objective of this paper is to propose efficient methods for numerical solution of the Stokes equation with local Coulomb's slip boundary conditions in 3D. We present two computational strategies and compare their efficiency. Similar problem but in 2D has been analyzed in [21]. Thus the present paper can be considered to be its

extension to 3D case. However it should be pointed out that this extension is not straightforward, above all from the computational point of view as it will be seen later on.

The paper is organized as follows. Section 2 presents classical setting of the problem and its different weak formulations used in computations. To start with a continuous model is helpful for better understanding of their algebraic counterparts arising from finite element discretizations. The first strategy is based on the velocity–pressure formulation of the Stokes equation with local Coulomb's slip conditions. This is done only in a formal way from reasons exposed above. The second strategy uses a fixed-point approach. Instead of the Stokes system with Coulomb's law we solve a sequence of problems with the Tresca slip conditions. They define one iterative step of the method of successive approximations. The resulting normal stress σ_ν is used to update the slip bound in the next iteration. To obtain directly the approximation of σ_ν, the dualization of the impermeability condition is proposed. We utilize the fact that the Lagrange multiplier releasing this constraint is equal to σ_ν. Numerical realization is based on the four-field formulation of the problem with Coulomb's and Tresca's slip law, i.e. the formulation in terms of $\boldsymbol{u}$, p, $\boldsymbol{\sigma}_\tau$, and σ_ν. Section 3 is devoted to the mathematical analysis of the discretized three field formulation of the problem for $\boldsymbol{u}$, p, and σ_ν, i.e. keeping j in the original, nonsmooth form. A special attention is paid to the discretization of the fixed-point mapping. Its simple restriction on a relevant finite element space cannot be used since it does not map this space into itself. For this reason a "return" mapping has to be introduced. We formulate sufficient conditions on finite element spaces and the return mapping under which the discrete model has at least one solution for any discretization parameter h and any coefficient of friction $\mathscr{F}$. In addition, if $\mathscr{F}$ is small or large enough, then the solution is unique. However, wording "small/large enough" depends on the mutual relation between $\mathscr{F}$ and h, i.e. the condition is mesh dependent.

In computations we use the semi-smooth Newton method [14,24] for the Tresca model in context of the fixed-point approach or directly for solving the algebraic system arising from the Coulomb model. The slip conditions are equivalently expressed at each slip node by using the projection on the circle. The algebraic system for the Tresca model is modified using the approach as in [19]. Then resulting Schur complements are symmetric, positive definite and the conjugate gradient method can be used as the inner solver. On the other hand the situation is completely different for the semi-smooth Newton method applied directly to the Coulomb model. Just as in 2D [20,21], the Jacobians and the resulting Schur complements are non-symmetric and indefinite owing to the fact that the velocity formulation of the Stokes problem with local Coulomb slip cannot be equivalently expressed as a minimization of a functional, Moreover the Schur complements in 3D are more involved than in 2D due to the more complicated definition of the projection mapping. The respective linear systems defining steps of the Newton method are solved by the BiCGSTAB algorithm.

The paper uses following notation. Let Ξ be a bounded domain in $\mathbb{R}^n$, $n = 2, 3$. The symbol $H^k(\Xi)$, $k \geq 0$ integer, denotes the Sobolev space of functions defined in Ξ which are together with their generalized derivatives up to order k square integrable in Ξ. We set $H^0(\Xi) = L^2(\Xi)$. The scalar product in $L^2(\Xi)$, the norm in $H^k(\Xi)$ will be denoted by $(\cdot,\cdot)_{0,\Xi}$ and $\|\cdot\|_{k,\Xi}$, respectively. If X is an ordered vector space, the symbol X_+ stands for its subset of nonnegative elements. For vectors, matrices, vector valued functions and spaces we use bold characters. The scalar product of two vectors $\mathbf{a}, \mathbf{b} \in \mathbb{R}^m$ is denoted by $\mathbf{a} \cdot \mathbf{b}$ and their Euclidean norm by $\|\cdot\|$. The symbol $\mathbb{R}^{p\times q}$ stands for the space of $(p \times q)$ matrices. If $\mathbf{A} = (a_{ij}), \mathbf{B} = (b_{ij}) \in \mathbb{R}^{p\times q}$, then $\mathbf{A} : \mathbf{B} := a_{ij}b_{ij}$ using the summation convention. By $\mathbf{0}$ we denote the zero matrix or the zero vector and $\mathbf{I} \in \mathbb{R}^{p\times p}$ stands for the identity matrix. If $\mathbf{A} = (a_{ij}) \in \mathbb{R}^{p\times p}$, then $diag(\mathbf{A})$ denotes the corresponding diagonal matrix. If $\mathbf{a} = (a_1, \ldots, a_p) \in \mathbb{R}^p$, then $diag(\mathbf{a}) = diag(a_1, \ldots, a_p) \in \mathbb{R}^{p\times p}$ is the diagonal matrix with the diagonal represented by the vector $\mathbf{a}$. Calligraphic symbols will be used for index sets, for instance: $\mathscr{M} = \{1, 2, \ldots, p\}$. The indicator matrix of a subset $\mathscr{S} \subseteq \mathscr{M}$ is the diagonal matrix $\mathbf{I}_{\mathscr{S}} = diag(s_1, s_2, \ldots, s_p) \in \mathbb{R}^{p\times p}$, where $s_i = 1$ for $i \in \mathscr{S}$ and $s_i = 0$ if $i \notin \mathscr{S}$. Finally, the symbol c stands for a generic positive constant which may take different values at different places of its appearance. To emphasize that c depends on some parameters $l_1, \ldots, l_p$ we write $c := c(l_1, \ldots, l_p)$.

2. Classical and weak formulations of the problem

Let $\Omega \subset \mathbb{R}^3$ be a bounded domain with the Lipschitz boundary $\partial\Omega$ which is decomposed into two non-empty, non-overlapping parts Γ and S open in $\partial\Omega$: $\partial\Omega = \overline{\Gamma} \cup \overline{S}$, $\Gamma \cap S = \emptyset$. *The classical formulation* of the Stokes problem with the local Coulomb slip conditions on S reads as follows: find a velocity field $\boldsymbol{u} : \Omega \mapsto \mathbb{R}^3$ and a

pressure $p : \Omega \mapsto \mathbb{R}$ satisfying the following system of the differential equations in Ω and the boundary conditions on $\partial\Omega$:

$$\left.\begin{array}{rcll} -2\mu \operatorname{div} \mathbb{D}(\boldsymbol{u}) + \nabla p &=& \boldsymbol{f} & \text{in } \Omega, \\ \operatorname{div} \boldsymbol{u} &=& 0 & \text{in } \Omega, \\ \boldsymbol{u} &=& \boldsymbol{0} & \text{on } \Gamma, \\ u_\nu &=& 0 & \text{on } S, \\ \|\boldsymbol{\sigma}_\tau\| &\le& \mathscr{F}|\sigma_\nu| & \text{on } S, \\ \mathscr{F}|\sigma_\nu|\boldsymbol{u}_\tau &=& -\boldsymbol{\sigma}_\tau \|\boldsymbol{u}_\tau\| & \text{on } S, \end{array}\right\} \tag{2.1}$$

where $\boldsymbol{f} \in (L^2(\Omega))^3$ is a volume force acting on the fluid, $\mu > 0$ is a constant dynamic viscosity, $\mathbb{D}(\boldsymbol{u}) = 1/2\,(\nabla \boldsymbol{u} + (\nabla \boldsymbol{u})^T)$ is the symmetric part of $\nabla \boldsymbol{u}$ and $\mathscr{F} > 0$ is a constant slip coefficient. The velocity field $\boldsymbol{u}$ is decomposed into the normal and tangential part: $\boldsymbol{u} = u_\nu \boldsymbol{\nu} + \boldsymbol{u}_\tau$, $u_\nu := \boldsymbol{u} \cdot \boldsymbol{\nu}$, where $\boldsymbol{\nu}$ is the outward unit normal vector to $\partial\Omega$ and $\boldsymbol{u}_\tau \perp u_\nu \boldsymbol{\nu}$. Analogously, the stress vector $\boldsymbol{\sigma} = 2\mu\mathbb{D}(\boldsymbol{u})\boldsymbol{\nu} - p\boldsymbol{\nu}$ on $\partial\Omega$ will be decomposed into the normal and shear stress: $\boldsymbol{\sigma} = \sigma_\nu \boldsymbol{\nu} + \boldsymbol{\sigma}_\tau$, $\sigma_\nu := \boldsymbol{\sigma} \cdot \boldsymbol{\nu}$ and $\boldsymbol{\sigma}_\tau \perp \sigma_\nu \boldsymbol{\nu}$.

Last two conditions in (2.1) express the local Coulomb slip law on S: the Euclidean norm of $\boldsymbol{\sigma}_\tau$ cannot exceed the value $\mathscr{F}|\sigma_\nu|$ which depends on the solution of the problem itself. In addition, from $(2.1)_6$ it follows that a slip at $x \in S$, i.e. $\boldsymbol{u}_\tau(x) \neq \boldsymbol{0}$ occurs only if $\|\boldsymbol{\sigma}_\tau(x)\| = \mathscr{F}|\sigma_\nu(x)|$ and the vectors $\boldsymbol{u}_\tau$ and $\boldsymbol{\sigma}_\tau$ have the opposite directions at x.

Below we present several weak formulations of (2.1) which will be used in subsequent parts of the paper in computations. To this end we introduce function spaces and forms:[1]

$$\left.\begin{array}{ll} \boldsymbol{W}(\Omega) = \{\boldsymbol{v} \in (H^1(\Omega))^3 |\ \boldsymbol{v} = \boldsymbol{0} \text{ on } \Gamma\}, & \\ \boldsymbol{V}(\Omega) = \{\boldsymbol{v} \in \boldsymbol{W}(\Omega) |\ v_\nu = 0 \text{ on } S\}, & \\ Q(\Omega) = \{q \in L^2(\Omega) |\ \displaystyle\int_\Omega q \,\mathrm{d}x = 0\} & \\ a(\boldsymbol{u}, \boldsymbol{v}) = \displaystyle\int_\Omega \mathbb{D}\boldsymbol{u} : \mathbb{D}\boldsymbol{v} \,\mathrm{d}x, & \boldsymbol{u}, \boldsymbol{v} \in \boldsymbol{W}(\Omega) \\ b(\boldsymbol{v}, q) = \displaystyle\int_\Omega \operatorname{div} \boldsymbol{v} q \,\mathrm{d}x, & \boldsymbol{v} \in \boldsymbol{W}(\Omega),\ q \in Q(\Omega) \\ j(g, \|\boldsymbol{v}_\tau\|) = \mathscr{F} \displaystyle\int_S g\|\boldsymbol{v}_\tau\| \mathrm{d}s, & \boldsymbol{v} \in \boldsymbol{W}(\Omega),\ g \in L^2_+(S). \end{array}\right\} \tag{2.2}$$

We start with the *implicit variational formulation* (IVF) of (2.1). Multiplying $(2.1)_{1,2}$ by test functions $(\boldsymbol{v}, q) \in \boldsymbol{V}(\Omega) \times Q(\Omega)$, using the boundary conditions on S and Green's formula we obtain the following inequality type problem:

$$\left.\begin{array}{l} \text{Find } (\boldsymbol{u}, p) \in \boldsymbol{V}(\Omega) \times Q(\Omega) \text{ such that} \\ a(\boldsymbol{u}, \boldsymbol{v} - \boldsymbol{u}) - b(\boldsymbol{v} - \boldsymbol{u}, p) + j(|\sigma_\nu|, \|\boldsymbol{v}_\tau\|) - j(|\sigma_\nu|, \|\boldsymbol{u}_\tau\|) \ge (\boldsymbol{f}, \boldsymbol{v} - \boldsymbol{u})_{0,\Omega}, \quad \forall \boldsymbol{v} \in \boldsymbol{V}(\Omega) \\ b(\boldsymbol{u}, q) = 0, \quad \forall q \in Q(\Omega). \end{array}\right\} (\mathscr{P})_{\mathrm{IVF}}$$

Owing to the presence of $|\sigma_\nu|$ in the argument of j *we shall suppose here and in what follows that* $\sigma_\nu \in L^2(S)$. Recall that the existence of the solution to $(\mathscr{P})_{\mathrm{IVF}}$ remains (to our knowledge) still open.

Another possibility is the *fixed-point formulation* (FPF) of (2.1). The unknown slip bound $|\sigma_\nu|$ in $(\mathscr{P})_{\mathrm{IVF}}$ is now replaced by an arbitrary function $g \in L^2_+(S)$. The new problem reads as follows: given $g \in L^2_+(S)$,

$$\left.\begin{array}{l} \text{Find } (\boldsymbol{u}(g), p(g)) \in \boldsymbol{V}(\Omega) \times Q(\Omega) \text{ such that} \\ a(\boldsymbol{u}(g), \boldsymbol{v} - \boldsymbol{u}(g)) - b(\boldsymbol{v} - \boldsymbol{u}(g), p(g)) + j(g, \|\boldsymbol{v}_\tau\|) - j(g, \|\boldsymbol{u}_\tau(g)\|) \ge (\boldsymbol{f}, \boldsymbol{v} - \boldsymbol{u}(g))_{0,\Omega}, \quad \forall \boldsymbol{v} \in \boldsymbol{V}(\Omega) \\ b(\boldsymbol{u}(g), q) = 0, \quad \forall q \in Q(\Omega). \end{array}\right\} (\mathscr{P}(g))$$

$(\mathscr{P}(g))$ is the weak formulation of the Stokes problem with the Tresca slip conditions on S in which the function $g \in L^2_+(S)$ represents the *known* slip bound. Such problem has a unique solution for any $g \in L^2_+(S)$ [15]. As before

[1] Here and in what follows we set $2\mu = 1$.

we suppose that the corresponding normal stress $\sigma_\nu(g)$ *belongs to* $L^2(S)$ *for any* $g \in L^2_+(S)$. This enables us to define the mapping $\Psi : L^2_+(S) \to L^2_+(S)$ by

$$\Psi(g) = |\sigma_\nu(g)| \qquad \forall g \in L^2_+(S)\,. \tag{2.3}$$

From the definitions of $(\mathscr{P})_{\rm IVF}$ and $(\mathscr{P}(g))$ we see that $(\boldsymbol{u}, p)$ solves $(\mathscr{P})_{\rm IVF}$ if and only if $(\boldsymbol{u}, p) = (\boldsymbol{u}(|\sigma_\nu|), p(|\sigma_\nu|))$ solves $(\mathscr{P}(|\sigma_\nu|))$, where σ_ν is the normal stress corresponding to $(\boldsymbol{u}, p)$. In other words

$$\Psi(|\sigma_\nu|) = |\sigma_\nu| \text{ on } S\,. \qquad (\mathscr{P})_{\rm FPF}$$

To find fixed-points of Ψ one can use various methods (successive approximations, optimal control techniques, e.g.).

Problems $(\mathscr{P})_{\rm IVF}$ and $(\mathscr{P})_{\rm FPF}$ are nonsmooth due to the functional j. In addition, numerical realization of both problems needs a good approximation of the normal stress σ_ν. To handle these difficulties we use duality approaches to regularize problems and to release the impermeability condition $v_\nu = 0$ on S.

From the definition of $(\mathscr{P}(g))$, $g \in L^2_+(S)$ we see that the velocity vector $\boldsymbol{u}(g)$ satisfies the following variational inequality:

$$\begin{aligned}&\text{Find } \boldsymbol{u}(g) \in \boldsymbol{V}_0(\Omega) \text{ such that}\\ &a(\boldsymbol{u}(g), \boldsymbol{v} - \boldsymbol{u}(g)) + j(g, \|\boldsymbol{v}_\tau\|) - j(g, \|\boldsymbol{u}_\tau(g)\|) \geq (\boldsymbol{f}, \boldsymbol{v} - \boldsymbol{u}(g))_{0,\Omega}, \quad \forall \boldsymbol{v} \in \boldsymbol{V}_0(\Omega)\end{aligned} \tag{2.4}$$

or equivalently

$$\boldsymbol{u}(g) = \arg\,\min\{J(\boldsymbol{v}) + j(g, \|\boldsymbol{v}_\tau\|),\ \boldsymbol{v} \in \boldsymbol{V}_0(\Omega)\}\,,$$

where

$$\boldsymbol{V}_0(\Omega) = \{\boldsymbol{v} \in \boldsymbol{V}(\Omega) \mid \operatorname{div} \boldsymbol{v} = 0 \text{ in } \Omega\}$$

and

$$J(\boldsymbol{v}) = \frac{1}{2}\, a(\boldsymbol{v}, \boldsymbol{v}) - (\boldsymbol{f}, \boldsymbol{v})_{0,\Omega}\,.$$

Let

$$\left.\begin{aligned} X_\nu &= \{\varphi \in L^2(S) \mid \exists \boldsymbol{v} \in \boldsymbol{W}(\Omega) : \varphi = v_\nu \text{ on } S\},\ X'_\nu = \text{dual of } X_\nu,\\ \boldsymbol{K}(\mathscr{F}g) &= \{\boldsymbol{\omega} \in (L^2(S))^2 \mid \|\boldsymbol{\omega}\| \leq \mathscr{F}g \text{ a.e. on } S\},\ g \in L^2_+(S)\,.\end{aligned}\right\} \tag{2.5}$$

It is easy to see that

$$j(g, \|\boldsymbol{v}_\tau\|) = \mathscr{F} \int_S g\, \|\boldsymbol{v}_\tau\|\, \mathrm{d}s = \sup_{\boldsymbol{\omega} \in \boldsymbol{K}(\mathscr{F}g)} \int_S \boldsymbol{\omega} \cdot \boldsymbol{v}_\tau\, \mathrm{d}s$$

and

$$\sup_{\lambda \in X'_\nu} \langle \lambda, v_\nu \rangle \in \{0, \infty\}\,, \quad \boldsymbol{v} \in \boldsymbol{W}(\Omega)\,,$$

where $\langle , \rangle$ stands for the duality pairing between X'_ν and X_ν, is the indicator function of $\boldsymbol{V}(\Omega)$. Hence

$$\min_{\boldsymbol{v} \in \boldsymbol{V}_0(\Omega)} \{J(\boldsymbol{v}) + j(g, \|\boldsymbol{v}_\tau\|)\} = \min_{\boldsymbol{v} \in \boldsymbol{W}(\Omega)} \sup_{q \in Q(\Omega)} \sup_{\substack{\lambda \in X'_\nu \\ \boldsymbol{\omega} \in \boldsymbol{K}(\mathscr{F}g)}} \mathscr{L}(\boldsymbol{v}, q, \boldsymbol{\omega}, \lambda),$$

where $\mathscr{L} : \boldsymbol{Z}(\mathscr{F}g) := \boldsymbol{W}(\Omega) \times Q(\Omega) \times \boldsymbol{K}(\mathscr{F}g) \times X'_\nu \to \mathbb{R}$ is the Lagrangian defined by

$$\mathscr{L}(\boldsymbol{v}, q, \boldsymbol{\omega}, \lambda) = J(\boldsymbol{v}) - b(\boldsymbol{v}, q) - (\boldsymbol{\omega}, \boldsymbol{v}_\tau)_{0,S} - \langle \lambda, v_\nu \rangle.$$

The *mixed formulation* of $(\mathscr{P}(g))$ is given by the following saddle-point problem for $\mathscr{L}$:

$$\left.\begin{aligned}&\text{Find } (\boldsymbol{u}^*(g), p^*(g), \boldsymbol{\omega}^*(g), \lambda^*(g)) \in \boldsymbol{Z}(\mathscr{F}g) \text{ such that}\\ &\mathscr{L}(\boldsymbol{u}^*(g), q, \boldsymbol{\omega}, \lambda) \leq \mathscr{L}(\boldsymbol{u}^*(g), p^*(g), \boldsymbol{\omega}^*(g), \lambda^*(g)) \leq \mathscr{L}(\boldsymbol{v}, p^*(g), \boldsymbol{\omega}^*(g), \lambda^*(g)) \quad \forall (\boldsymbol{v}, q, \boldsymbol{\omega}, \lambda) \in \boldsymbol{Z}(\mathscr{F}g)\end{aligned}\right\}$$

or equivalently

$$\left.\begin{array}{rll} \text{Find } (\boldsymbol{u}^*(g), p^*(g), \boldsymbol{\omega}^*(g), \lambda^*(g)) \in \boldsymbol{Z}(\mathscr{F}g) \text{ such that} & & \\ a(\boldsymbol{u}^*(g), \boldsymbol{v}) - b(\boldsymbol{v}, p^*(g)) - (\boldsymbol{\omega}^*(g), \boldsymbol{v}_\tau)_{0,S} - \langle \lambda^*(g), v_\nu\rangle & = (\boldsymbol{f}, \boldsymbol{v})_{0,\Omega} & \forall \boldsymbol{v} \in \boldsymbol{W}(\Omega) \\ b(\boldsymbol{u}^*(g), q) & = 0 & \forall q \in Q(\Omega) \\ \langle \lambda, u_\nu^*(g)\rangle & = 0 & \forall \lambda \in X_\nu' \\ (\boldsymbol{\omega} + \boldsymbol{\omega}^*(g), \boldsymbol{u}_\tau^*(g))_{0,S} & \le 0 & \forall \boldsymbol{\omega} \in \boldsymbol{K}(\mathscr{F}g). \end{array}\right\} (\mathscr{M}(g))$$

It is easy to verify [23] that there exists a unique quadruplet in $\boldsymbol{Z}(\mathscr{F}g)$ solving $(\mathscr{M}(g))$, namely $(\boldsymbol{u}^*(g), p^*(g), \boldsymbol{\omega}^*(g), \lambda^*(g)) = (\boldsymbol{u}(g), p(g), \boldsymbol{\sigma}_\tau(g), \sigma_\nu(g))$, where $(\boldsymbol{u}(g), p(g))$ solves $(\mathscr{P}(g))$, $\boldsymbol{\sigma}_\tau(g), \sigma_\nu(g)$ is the shear, and normal stress corresponding to $(\boldsymbol{u}(g), p(g))$, respectively. The functional Ψ defined by (2.3) can be also expressed as follows:

$$\Psi(g) = |\lambda^*(g)| \text{ on } S\,. \tag{2.6}$$

The *mixed formulation* of $(\mathscr{P})_{\mathrm{IVF}}$ is obtained from $(\mathscr{M}(g))$, replacing $g \in L^2_+(S)$ by $|\lambda^*|$, i.e.

$$\left.\begin{array}{rll} \text{Find } (\boldsymbol{u}^*, p^*, \boldsymbol{\omega}^*, \lambda^*) \in \boldsymbol{Z}(\mathscr{F}|\lambda^*|) \text{ such that} & & \\ a(\boldsymbol{u}^*, \boldsymbol{v}) - b(\boldsymbol{v}, p^*) - (\boldsymbol{\omega}^*, \boldsymbol{v}_\tau)_{0,S} - \langle \lambda^*, v_\nu\rangle & = (\boldsymbol{f}, \boldsymbol{v})_{0,\Omega} & \forall \boldsymbol{v} \in \boldsymbol{W}(\Omega) \\ b(\boldsymbol{u}^*, q) & = 0 & \forall q \in Q(\Omega) \\ \langle \lambda, u_\nu^*\rangle & = 0 & \forall \lambda \in X_\nu' \\ (\boldsymbol{\omega} + \boldsymbol{\omega}^*, \boldsymbol{u}_\tau^*)_{0,S} & \le 0 & \forall \boldsymbol{\omega} \in \boldsymbol{K}(\mathscr{F}|\lambda^*|). \end{array}\right\} (\mathscr{M})_{\mathrm{IVF}}$$

Providing that a solution $(\boldsymbol{u}, p)$ to $(\mathscr{P})$ exists, the quadruplet $(\boldsymbol{u}^*, p^*, \boldsymbol{\omega}^*, \lambda^*) = (\boldsymbol{u}, p, \boldsymbol{\sigma}_\tau, \sigma_\nu)$, where $\boldsymbol{\sigma}_\tau, \sigma_\nu$ is the shear, and normal stress on S corresponding to $(\boldsymbol{u}, p)$, respectively.

Remark 2.1. The pressure component p of the solution to $(\mathscr{M}(g))$ under the boundary conditions $(2.1)_{3-6}$ is unique in the space $Q(\Omega)$. On the other hand, p as the element of $L^2(\Omega)$ is determined up to an arbitrary additive constant c. We overcome this drawback by adding a supplementary boundary condition to the existing ones. The condition will be chosen in such a way that problem $(\mathscr{M}(g))$ is uniquely solvable in $\boldsymbol{W}(\Omega) \times L^2(\Omega)$. To this end the boundary $\partial\Omega$ will be split into *three* non-empty, non-overlapping parts Γ, S and Γ_N open in $\partial\Omega$. We keep the conditions $(2.1)_{3-6}$ on Γ, and S while the value of the stress vector σ will be prescribed on Γ_N: $\sigma = \overline{\sigma} \in (L^2(\Gamma_N))^3$ given. The weak formulations of the problem remain practically unchanged just with the following minor modification: the right hand side $(\boldsymbol{f}, \boldsymbol{v})_{0,\Omega}$ has to be now replaced by the linear form $l(\boldsymbol{v}) = (\boldsymbol{f}, \boldsymbol{v})_{0,\Omega} + (\overline{\sigma}, \boldsymbol{v})_{0,\Gamma_N}$. This way will be used in model examples presented in Section 6.

Remark 2.2. If problem $(\mathscr{P})_{\mathrm{IVF}}$ has a solution $(\boldsymbol{u}, p)$ such that the corresponding normal and shear stresses satisfy $\sigma_\nu \neq 0$ and $\|\boldsymbol{\sigma}_\tau\| < \mathscr{F}|\sigma_\nu|$ a.e. on S then $\boldsymbol{u}_\tau = \boldsymbol{0}$. This together with $(2.1)_4$ yields $\boldsymbol{u} = \boldsymbol{0}$ a.e.on S. Thus $(\boldsymbol{u}, p)$ is the unique solution in $W(\Omega) \times Q(\Omega)$ to the Stokes system with the no-slip boundary condition on $\partial\Omega$. In addition, the same pair $(\boldsymbol{u}, p)$ solves $(\mathscr{P})_{\mathrm{IVF}}$ for any slip coefficient $\mathscr{F}^+ > \mathscr{F}$.

3. Existence/unicity of solutions to discretized problems

The aim of this section is to establish and analyze the discrete fixed-point formulation $(\mathscr{P})_{\mathrm{FPF}}$. From these results we obtain information on the existence and possible uniqueness of the solution to the *discretized* Stokes problem with Coulomb's slip conditions on S. We use a slightly modified mixed formulation $(\mathscr{M}(g))$ involving only one Lagrange multiplier on S which releases the impermeability condition $v_\nu = 0$ on S but keeping the original nonsmooth form of the functional j.

Let $\boldsymbol{W}_h(\Omega) \subset \boldsymbol{W}(\Omega)$, $Q_h(\Omega) \subset Q(\Omega)$ be finite element subspaces of $\boldsymbol{W}(\Omega)$, and $Q(\Omega)$, respectively, where $h > 0$ stands for a discretization parameter (a mesh norm, e.g.), dim $\boldsymbol{W}_h(\Omega) = n := n(h)$, dim $Q_h(\Omega) = m := m(h)$, and $n(h),\ m(h) \to \infty$ as $h \to 0+$. The discretization of X_ν is given by

$$X_{h\nu} = \{\varphi_h : S \mapsto \mathbb{R} \mid \exists\ \boldsymbol{v}_h \in \boldsymbol{W}_h(\Omega) : \varphi_h = v_{h\nu} \text{ on } S\}. \tag{3.1}$$

Next, we shall suppose that $X_{h\nu} \subset H_0^1(S)$. This assumption is not restrictive, since $\boldsymbol{W}_h(\Omega)$ consists of continuous, piecewise polynomial functions in $\overline{\Omega}$ and S is supposed to be sufficiently smooth. To simplify our presentation *we*

assume that S is flat, i.e. the unit normal vector $\boldsymbol{\nu}$ is constant on S. Finally, the dual space X_ν' will be discretized by finite element subspaces M_H of $L^2(S)$, where $H > 0$ stands for (possible) another discretization parameter, $\dim M_H = r := r(H) \to \infty$ as $H \to 0+$. Recall that M_{H+} denotes the cone of nonnegative elements of M_H.

In what follows we suppose that the pairs $\{\boldsymbol{W}_h(\Omega),\ Q_h(\Omega)\}$ and $\{X_{h\nu},\ M_H\}$ satisfy the following Babuška–Brezzi conditions:

- $\exists\ \beta_1 = \text{const.} > 0$ independent of h such that

$$\sup_{\boldsymbol{v}_h \in \boldsymbol{W}_h(\Omega)\setminus\{\boldsymbol{0}\}} \frac{b(\boldsymbol{v}_h, q_h)}{\|\boldsymbol{v}_h\|_{1,\Omega}} \geq \beta_1 \|q_h\|_{0,\Omega} \qquad \forall q_h \in Q_h(\Omega)\,, \tag{3.2}$$

- $\exists\ \beta_2 = \text{const.} > 0$ independent of h, H such that

$$\sup_{\boldsymbol{v}_h \in \boldsymbol{W}_h(\Omega)\setminus\{\boldsymbol{0}\}} \frac{(\mu_H, v_{h\nu})_{0,S}}{\|\boldsymbol{v}_h\|_{1,\Omega}} \geq \beta_2 \|\mu_H\|_{-1/2,S} \qquad \forall \mu_H \in M_H\,, \tag{3.3}$$

where

$$\|\mu_H\|_{-1/2,S} = \sup_{\boldsymbol{v} \in \boldsymbol{W}(\Omega)\setminus\{\boldsymbol{0}\}} \frac{(\mu_H, v_\nu)_{0,S}}{\|\boldsymbol{v}\|_{1,\Omega}}\,.$$

The *discrete mixed formulation* of the Stokes problem with the Tresca slip conditions on S reads as follows: given $g_H \in M_{H+}$,

$$\left.\begin{aligned} &\text{Find } (\boldsymbol{u}_h(g_H), p_h(g_H), \lambda_H(g_H)) \in \boldsymbol{W}_h(\Omega) \times Q_h(\Omega) \times M_H \text{ such that} \\ &a(\boldsymbol{u}_h(g_H), \boldsymbol{v}_h - \boldsymbol{u}_h(g_H)) - b(\boldsymbol{v}_h - \boldsymbol{u}_h(g_H), p_h(g_H)) - (\lambda_H(g_H), v_{h\nu} - u_{h\nu}(g_H))_{0,S} \\ &\quad + j(g_H, \|\boldsymbol{v}_{h\tau}\|) - j(g_H, \|\boldsymbol{u}_{h\tau}\|) \geq (\boldsymbol{f}, \boldsymbol{v}_h - \boldsymbol{u}_h(g_H))_{0,\Omega} \qquad \forall \boldsymbol{v}_h \in \boldsymbol{W}_h(\Omega) \\ &b(\boldsymbol{u}_h(g_H), q_h) = 0 \quad \forall q_h \in Q_h(\Omega) \\ &(\mu_H, u_{h\nu})_{0,S} = 0 \quad \forall \mu_H \in M_H\,. \end{aligned}\right\} (\mathscr{M}(g_H))_h$$

The existence and uniqueness of the solution to $(\mathscr{M}(g_H))_h$ for any $g_H \in M_{H+}$ follows from (3.2), (3.3) and ellipticity of the bilinear form a. Moreover, there exists a constant $c := c(\|\boldsymbol{f}\|_{0,\Omega}, \beta_1, \beta_2) > 0$ which does not depend on h, H, $\mathscr{F}$ and $g_H \in M_{H+}$ such that

$$\|\boldsymbol{u}_h(g_H)\|_{1,\Omega} + \|p_h(g_H)\|_{0,\Omega} + \|\lambda_H(g_H)\|_{-1/2,S} \leq c\,. \tag{3.4}$$

Let us recall that $\lambda_H(g_H)$ represents the discrete normal stress on S. To define the discretization of $(\mathscr{P})_{\mathrm{FPF}}$ one needs to discretize the functional Ψ from (2.6). Since the space M_H consists of piecewise polynomial functions on a given partition of S, the implication

$$\mu_H \in M_H \implies |\mu_H| \in M_{H+} \qquad \forall \mu_H \in M_H\,, \tag{3.5}$$

holds true for piecewise constant functions but not for higher order polynomials. Thus a simple restriction of Ψ on M_H cannot be used in the discrete fixed-point formulation.

For this reason we introduce a linear mapping $\mathscr{R}_H : H^1(S) \cap C(\overline{S}) \to M_H$ with the following properties:

$$\mathscr{R}_H(|\mu_H|) \in M_{H+} \qquad \forall \mu_H \in M_H \tag{3.6}$$

$$\|\mathscr{R}_H(|\mu_H|)\|_{0,S} \leq c\,\|\mu_H\|_{0,S} \quad \forall \mu_H \in M_H \tag{3.7}$$

where $c := \text{const.} > 0$ is independent of H.

If (3.5) is satisfied we simply set $\mathscr{R}_H = id$. Finally we suppose that elements of M_H satisfy the following inverse inequality: there exists a constant $c > 0$ which does not depend on H such that

$$\|\mu_H\|_{0,S} \leq c H^{-1/2}\,\|\mu_H\|_{-1/2,S} \quad \forall \mu_H \in M_H\,. \tag{3.8}$$

The discrete form Ψ_H of Ψ is defined by

$$\Psi_H : M_{H+} \to M_{H+},\ \ \Psi_H(g_H) = \mathscr{R}_H(|\lambda_H(g_H)|)\ \forall g_H \in M_{H+}\,, \tag{3.9}$$

where $\lambda_H(g_H) \in M_H$ is the last component of the solution to $(\mathscr{M}(g_H))_h$.

Definition 3.1. By a solution to the discretized Stokes problem with local Coulomb's slip law we mean any solution $(\boldsymbol{u}_h(g_H^*), p_h(g_H^*), \lambda_H(g_H^*))$ to $(\mathscr{M}(g_H^*))_h$ with $g_H^* \in M_{H+}$ being a fixed-point of Ψ_H.

First we prove the following existence result.

Theorem 3.1. *Let (3.7) and (3.8) be satisfied. Then Ψ_H defined by (3.9) has at least one fixed-point for any h, H and any slip coefficient $\mathscr{F}$. All fixed-points lie in the ball $\mathscr{B}_H = \{\mu_H \in M_{H+} \mid \|\mu_H\|_{0,S} \le cH^{-1/2}\}$, where $c := const. > 0$ does not depend on h, H and $\mathscr{F}$.*

Proof. We use Brouwer's fixed-point theorem. Let $g_H \in M_{H+}$ be given. Then

$$\|\Psi_H(g_H)\|_{0,S} \overset{(3.9)}{=} \|\mathscr{R}_H(|\lambda_H(g_H)|)\|_{0,S} \overset{(3.7)}{\le} c\,\|\lambda_H(g_H)\|_{0,S} \overset{(3.8)}{\le} cH^{-1/2}\,\|\lambda_H(g_H)\|_{-1/2,S} \overset{(3.4)}{\le} cH^{-1/2}.$$

Hence $\Psi_H(\mathscr{B}_H) \subseteq \mathscr{B}_H$. Obviously, Ψ_H is continuous in M_{H+} in view of continuous dependence of the solution to $(\mathscr{M}(g_H))_h$ on $g_H \in M_{H+}$ which is easy to verify. □

Next we shall present conditions under which Ψ_H is *Lipschitz continuous* in M_{H+}. Besides (3.7) and (3.8) we shall suppose that there exists a constant $c > 0$ which does not depend on H such that

$$|\mathscr{R}_H(|\mu_H|) - \mathscr{R}_H(|\overline{\mu}_H|)| \le c\mathscr{R}_H(|\mu_H - \overline{\mu}_H|) \text{ a.e. on } S \tag{3.10}$$

holds for every $\mu_H, \overline{\mu}_H \in M_H$.

Theorem 3.2. *Let (3.7), (3.8) and (3.10) be satisfied. Then the mapping Ψ_H defined by (3.9) is Lipschitz continuous in M_{H+}:*

$$\left\|\Psi_H(g_H) - \Psi_H(\overline{g}_H)\right\|_{0,S} \le c\mathscr{F}H^{-1/2}\left\|g_H - \overline{g}_H\right\|_{0,S} \quad \forall g_H, \overline{g}_H \in M_{H+}, \tag{3.11}$$

where $c > 0$ does not depend on $h, H, \boldsymbol{f}$ and $\mathscr{F}$.

Proof. Let $g_H, \overline{g}_H \in M_{H+}$ be given. Then

$$\begin{aligned}\left\|\Psi_H(g_H) - \Psi_H(\overline{g}_H)\right\|_{0,S} &= \left\|\mathscr{R}_H(|\lambda_H(g_H)|) - \mathscr{R}_H(|\lambda_H(\overline{g}_H)|)\right\|_{0,S} = \left\|\,|\mathscr{R}_H(|\lambda_H(g_H)|) - \mathscr{R}_H(|\lambda_H(\overline{g}_H)|)|\,\right\|_{0,S} \\ &\overset{(3.10)}{\le} c\left\|\mathscr{R}_H(|\lambda_H(g_H) - \lambda_H(\overline{g}_H)|)\right\|_{0,S} \overset{(3.7)}{\le} c\left\|\lambda_H(g_H) - \lambda_H(\overline{g}_H)\right\|_{0,S} \overset{(3.8)}{\le} cH^{-1/2}\left\|\lambda_H(g_H) - \lambda_H(\overline{g}_H)\right\|_{-1/2,S}\end{aligned} \tag{3.12}$$

To handle the last term in (3.12) we subtract $(\mathscr{M}(\overline{g}_H))_h$ from $(\mathscr{M}(g_H))_h$. We easily obtain the following estimate of the distance between their solutions:

$$\left\|\boldsymbol{u}_h(g_H) - \boldsymbol{u}_h(\overline{g}_H)\right\|_{1,\Omega} + \left\|p_h(g_H) - p_h(\overline{g}_H)\right\|_{0,\Omega} + \left\|\lambda_H(g_H) - \lambda_H(\overline{g}_H)\right\|_{-1/2,S} \le c\mathscr{F}\left\|g_H - \overline{g}_H\right\|_{0,S}$$

where $c > 0$ does not depend on $\boldsymbol{f}, h, H$ and $\mathscr{F}$ making use of ellipticity of a, (3.2) and (3.3). From this and (3.12) we arrive at the assertion of the theorem. □

Consequence 3.1. *If $c\mathscr{F}H^{-1/2} < 1$ in (3.11), then the mapping Ψ_H is contractive. Thus Ψ_H has a unique fixed-point and the method of successive approximations is convergent for any choice of the initial approximation $g_H^{(0)} \in M_{H+}$. Each iterative step is represented by the Stokes system with the Tresca slip conditions on S.*

In the rest of this section we present the spaces $\boldsymbol{W}_h(\Omega)$, $Q_h(\Omega)$, M_H and the mapping $\mathscr{R}_H$ which satisfy the conditions (3.2)–(3.8) and will be used in the computational part of the paper.

We shall suppose that $\Omega \subset \mathbb{R}^3$ is a *polyhedral* domain. Let $\{\mathscr{T}_h\}$ be a *regular* system of partitions of $\overline{\Omega}$ into polyhedra T with standard assumptions on their mutual position [9]. The pair $\{\boldsymbol{W}_h(\Omega), Q_h(\Omega)\}$ will be constructed by the P1+bubble/P1-elements:

$$\left.\begin{aligned}\boldsymbol{W}_h(\Omega) = &\quad \{\boldsymbol{v}_h \in \boldsymbol{W}(\Omega) \mid \boldsymbol{v}_{h|_T} \in (P_1(T))^3 \oplus (B(T))^3 \quad \forall T \in \mathscr{T}_h\} \\ Q_h(\Omega) = &\quad \{q_h \in C(\overline{\Omega}) \mid q_{h|_T} \in P_1(T) \quad \forall T \in \mathscr{T}_h,\ \int_\Omega q_h \mathrm{d}x = 0\},\end{aligned}\right\} \tag{3.13}$$

where $P_1(T)$ stands for the space of affine functions on T and $B(T)$ denotes the space of bubble functions of degree 3 on T. It is well-known that the pair $\{\boldsymbol{W}_h(\Omega), Q_h(\Omega)\}$ satisfies the Babuška–Brezzi condition (3.2) [8]. The

polyhedral meshing $\mathscr{T}_h$ of $\overline{\Omega}$ generates the triangulation $\mathscr{D}_h = \mathscr{T}_{h|_S}$ of $\overline{S}$. From the definition of $\boldsymbol{W}_h(\Omega)$ and the assumption on S it is readily seen that

$$X_{hv} = \{\varphi_h \in C(\overline{S}) |\ \varphi_{h|_K} \in P_1(K) \quad \forall K \in \mathscr{D}_h,\ \varphi_h = 0 \text{ on } \partial S\}\,. \tag{3.14}$$

The space M_H will be constructed by piecewise linear functions on $\mathscr{D}_h$ vanishing on ∂S. Then M_H coincides with X_{hv} and only one discretization parameter h is needed. We may assume that the pair $\{X_{hv}, X_{hv}\}$ satisfies the Babuška–Brezzi condition (3.3). Indeed, it is readily seen that the implication

$$\mu_h \in X_{hv}\ :\ (\mu_h, v_{hv})_{0,S} = 0\ \ \forall \boldsymbol{v}_h \in \boldsymbol{W}_h(\Omega) \implies \mu_h = 0 \tag{3.15}$$

is true. Hence (3.3) holds with a constant $\beta_2 > 0$, which however may depend on h. To show that β_2 can be chosen to be independent of h, one can use the stability in $H^1(S)$ of the L^2-projection on the space X_{hv}. This property has been proven in [7], e.g., for any spatial dimension under appropriate mesh conditions. Since (3.6) is not satisfied by functions from X_{hv} which change the sign in the interior of at least one triangle $K \in \mathscr{D}_h$, a mapping $\mathscr{R}_h\ :\ C(\overline{S}) \to X_{hv}$ is needed. We define

$$(\mathscr{R}_h v)_{|K} = P_1\text{-Lagrange interpolation of } v_{|K} \quad \forall K \in \mathscr{D}_h,\ \ v \in C(\overline{S})\,.$$

From its definition and properties of P_1-elements it follows that (3.6) and (3.10) with $c = 1$ are satisfied. Next we shall suppose that the system of triangulations $\{\mathscr{D}_h\}$ is *strongly regular* which justifies the use of inverse inequalities, in particular (3.8). It remains to prove (3.7). We have:

$$\|\mathscr{R}_h(|\mu_h|)\|_{0,S} \le \|\mathscr{R}_h(|\mu_h|) - |\mu_h|\,\|_{0,S} + \|\,|\mu_h|\,\|_{0,S} \le c h^s\,\|\,|\mu_h|\,\|_{s,S} + \|\mu_h\|_{0,S} \le c\,\|\mu_h\|_{0,S} + \|\mu_h\|_{0,S}\ ,$$

where $s \in (1, 3/2)$ and $c := \text{const.} > 0$ which does not depend on h. Here we used interpolation properties of $\mathscr{R}_h$, the fact that $|\mu_h| \in H^s(S)$, $s \in (1, 3/2)$ for any $\mu_h \in X_{hv}$ and the inverse inequality between $L^2(S)$ and $H^s(S)$. Further, the inequality $\||\mu_h|\|_{s,S} \le \|\mu_h\|_{s,S}$ follows from the definition of the norm in $H^s(S)$ for $s > 0$ non-integer [30]. Thus all the assumptions of Theorems 3.1 and 3.2 are verified. Let us note that, the impermeability condition on S is satisfied exactly on S as follows from (3.15).

4. Algebraic formulations

This section is devoted to the presentation of the algebraic formulations of the Stokes system with the Tresca and Coulomb slip conditions discretized by a mixed finite element method.

Let $\mathscr{T}_h$ denote a partition of a bounded polyhedral domain Ω into a finite number of polyhedra T with usual assumptions on their mutual position. Each $\mathscr{T}_h$ will be characterized by the following parameters: n_u, n_b, n_p, and n_s, where n_u = the total number (t.n.) of the vertices of $T \in \mathscr{T}_h$ belonging to $\overline{\Omega} \setminus \overline{\Gamma}$, n_b = t.n. of the polyhedra $T \in \mathscr{T}_h$, n_p = t.n. of the vertices of $T \in \mathscr{T}_h$ in $\overline{\Omega}$, and n_s = t.n. of the nodes of $\mathscr{T}_h$ in $\overline{S} \setminus \overline{\Gamma}$. These parameters determine the scale of the algebraic system. The velocity field $\boldsymbol{u}$ and the pressure p are discretized using the pair $\boldsymbol{W}_h(\Omega)$, $Q_h(\Omega)$ defined in (3.13). Thus the discrete velocity vector $\mathbf{u} \in \mathbb{R}^{3(n_u+n_b)}$ and the discrete pressure $\mathbf{p} \in \mathbb{R}^{n_p}$. In the sequel however all components of $\mathbf{u}$ which correspond to the bubble functions will be eliminated in advance on the element level. Consequently, the resulting vector $\mathbf{u}$ will be understood as an element of $\mathbb{R}^{3n_u}$ in what follows. The impermeability condition prescribed on the slip boundary will be released by the Lagrange multipliers from the space $M_h = X_{hv}$ defined in (3.14).

Let $g_h \in M_{h+}$ be given and consider the problem[2]

$$\left.\begin{array}{rll} \text{Find } (\boldsymbol{u}_h, p_h, \lambda_h) \in \boldsymbol{W}_h(\Omega) \times Q_h(\Omega) \times M_h \text{ such that} & & \\ a(\boldsymbol{u}_h, \boldsymbol{v}_h - \boldsymbol{u}_h) - b(\boldsymbol{v}_h - \boldsymbol{u}_h, p_h) - (\lambda_h, v_{hv} - u_{hv})_{0,S} & & \\ \quad + j_h(g_h, \|\boldsymbol{v}_{h\tau}\|) - j_h(g_h, \|\boldsymbol{u}_{h\tau}\|) & \ge (\boldsymbol{f}, \boldsymbol{v}_h - \boldsymbol{u}_h)_{0,\Omega} & \forall \boldsymbol{v}_h \in \boldsymbol{W}_h(\Omega) \\ b(\boldsymbol{u}_h, q_h) & = 0 & \forall q_h \in Q_h(\Omega) \\ (\mu_h, u_{hv})_{0,S} & = 0 & \forall \mu_h \in M_h\,. \end{array}\right\} \tag{4.1}$$

The symbol j_h stands for an approximation of j by an appropriate numerical integration formula.

Before we give the algebraic formulation of (4.1) we introduce several notation. By $\{a_i\}$, $i \in \mathscr{N} = \{1, \dots, n_s\}$ we denote the slip nodes, i.e. the nodes of $\mathscr{T}_h$ lying in $\overline{S} \setminus \overline{\Gamma}$. To express slip conditions, we use the local

[2] To simplify notation here and in what follows, the dependence of $(\boldsymbol{u}_h, p_h, \lambda_h)$ on g_h is not explicitly quoted.

orthogonal coordinate systems generated by the triplets $\{\boldsymbol{\nu}, \boldsymbol{\tau}_1, \boldsymbol{\tau}_2\}$ with origin at a_i, $i \in \mathcal{N}$ and define the full row rank $(n_s \times 3n_u)$ matrices $\mathbf{T}_1$, $\mathbf{T}_2$, $\mathbf{N}$ whose rows consist of the tangential, normal vectors $\boldsymbol{\tau}_1$, $\boldsymbol{\tau}_2$, and $\boldsymbol{\nu}$, respectively. If $\mathbf{a} \in \mathbb{R}^n$, then its ith component will be denoted by $(\mathbf{a})_i$. Finally, if $\mathbf{a} = (\mathbf{a}_1, \mathbf{a}_2) \in \mathbb{R}^{n_s} \times \mathbb{R}^{n_s}$ then ${}^i\mathbf{a} = ((\mathbf{a}_1)_i, (\mathbf{a}_2)_i) \in \mathbb{R}^2$. To define j_h we use the following integration rule on triangles $K \in \mathscr{D}_h$:

$$\int_K \varphi \approx \frac{1}{3}|K|(\varphi(i) + \varphi(j) + \varphi(k)), \quad \varphi \in C(K),$$

where $|K|$ = measure of K and i, j, k are the vertices of K. Using this formula for the evaluation of $j(g_h, \|\boldsymbol{\nu}_{h\tau}\|)$, $g_h \in M_{h+}$, $\boldsymbol{\nu}_h \in \boldsymbol{W}_h(\Omega)$ we obtain:

$$j(g_h, \|\boldsymbol{\nu}_{h\tau}\|) = \mathscr{F} \sum_{K \in \mathscr{D}_h} \int_K g_h \|\boldsymbol{\nu}_{h\tau}\| \approx \mathscr{F} \sum_{i=1}^{n_s} \omega_i g_i \|\boldsymbol{\nu}_{h\tau}(a_i)\|, \tag{4.2}$$

where $g_i := g_h(a_i)$, $\omega_i := |\operatorname{supp}(\varphi_i)|/3$ and φ_i is the Courant basis function associated with the slip node a_i, $i \in \mathcal{N}$. The last term in (4.2) defines the functional j_h appearing in (4.1). To get rid of $\|\boldsymbol{\nu}_{h\tau}(a_i)\|$ we use again the duality approach. To this end we introduce the following sets:

$$\mathbf{K}(\mathscr{F}\mathbf{g}) = \{\boldsymbol{\mu} = (\boldsymbol{\mu}_1, \boldsymbol{\mu}_2) \in \mathbb{R}^{n_s} \times \mathbb{R}^{n_s} \mid \|{}^i\boldsymbol{\mu}\| \le \mathscr{F} g_i, \ i \in \mathcal{N}\}, \tag{4.3}$$

and

$$\mathbf{K}_\omega(\mathscr{F}\mathbf{g}) = \{\boldsymbol{\mu} = (\boldsymbol{\mu}_1, \boldsymbol{\mu}_2) \in \mathbb{R}^{n_s} \times \mathbb{R}^{n_s} \mid \|{}^i\boldsymbol{\mu}\| \le \mathscr{F} g_i \omega_i, \ i \in \mathcal{N}\}, \tag{4.4}$$

where $\mathbf{g} = (g_1, \dots, g_{n_s})$.

Then

$$\begin{aligned} j_h(g_h, \|\boldsymbol{\nu}_{h\tau}\|) &= \max_{\boldsymbol{\mu} \in \mathbf{K}(\mathscr{F}\mathbf{g})} \sum_{i=1}^{n_s} \omega_i \, {}^i\boldsymbol{\mu} \cdot \boldsymbol{\nu}_{h\tau}(a_i) = \max_{\boldsymbol{\mu} \in \mathbf{K}_\omega(\mathscr{F}\mathbf{g})} \sum_{i=1}^{n_s} {}^i\boldsymbol{\mu} \cdot ((\mathbf{T}_1\mathbf{v})_i, (\mathbf{T}_2\mathbf{v})_i) \\ &= \max_{\boldsymbol{\mu} \in \mathbf{K}_\omega(\mathscr{F}\mathbf{g})} (\boldsymbol{\mu}_1 \cdot \mathbf{T}_1\mathbf{v} + \boldsymbol{\mu}_2 \cdot \mathbf{T}_2\mathbf{v}) = \max_{\boldsymbol{\mu} \in \mathbf{K}_\omega(\mathscr{F}\mathbf{g})} (\mathbf{T}_1^T\boldsymbol{\mu}_1 + \mathbf{T}_2^T\boldsymbol{\mu}_2) \cdot \mathbf{v} \end{aligned} \tag{4.5}$$

In the same way we express the duality term $(\lambda_h, v_{hv})_{0,S}$:

$$\begin{aligned} (\lambda_h, v_{hv})_{0,S} &= \sum_{K \in \mathscr{D}_h} \int_K \lambda_h v_{hv} \approx \sum_{i=1}^{n_s} \omega_i \lambda_h(a_i) v_{hv}(a_i) = \sum_{i=1}^{n_s} \omega_i (\mathbf{l}_v)_i (\mathbf{N}\mathbf{v})_i \\ &= \sum_{i=1}^{n_s} (\boldsymbol{\lambda}_v)_i (\mathbf{N}\mathbf{v})_i = \mathbf{N}^T\boldsymbol{\lambda}_v \cdot \mathbf{v}, \end{aligned} \tag{4.6}$$

where $(\mathbf{l}_v)_i = \lambda_h(a_i)$, $(\boldsymbol{\lambda}_v)_i = \omega_i(\mathbf{l}_v)_i$, $i \in \mathcal{N}$. The vector $\mathbf{l}_v \in \mathbb{R}^{n_s}$ consists of the nodal values of the discrete normal stress at the slip nodes a_i, $i \in \mathcal{N}$. The rescaled vector $\boldsymbol{\lambda}_v$ will be termed *the algebraic normal stress*. The same distinction will be used for the vectors $\mathbf{l}_\tau = (\mathbf{l}_{\tau_1}, \mathbf{l}_{\tau_2}) \in \mathbf{K}(\mathscr{F}\mathbf{g})$ representing the discrete shear stresses at a_i, $i \in \mathcal{N}$, while the rescaled vectors $\boldsymbol{\lambda}_\tau = (\boldsymbol{\lambda}_{\tau_1}, \boldsymbol{\lambda}_{\tau_2})$, where $(\boldsymbol{\lambda}_{\tau_j})_i = \omega_i(\mathbf{l}_{\tau_j})_i$, $i \in \mathcal{N}$, $j = 1, 2$ belong to $\mathbf{K}_\omega(\mathscr{F}\mathbf{g})$.

To avoid difficulties with non-uniqueness of p we proceed as in Remark 2.1, i.e. we introduce an additional Neumann type boundary condition on a part Γ_N. Using (4.5) and (4.6) we straightforwardly derive the algebraic form of the Lagrangian $\mathscr{L}$ introduced in Section 2 and define the saddle-point problem on $\mathbb{R}^{3n_u} \times \mathbf{K}_\omega(\mathscr{F}\mathbf{g}) \times \mathbb{R}^{n_s} \times \mathbb{R}^{n_p}$. The KKT-conditions characterizing the saddle-point problem lead to the following algebraic formulation of the discretized Stokes equation with the Tresca slip conditions:

$$\left.\begin{aligned} &\text{Find } (\mathbf{u}, (\boldsymbol{\lambda}_{\tau_1}, \boldsymbol{\lambda}_{\tau_2}), \boldsymbol{\lambda}_\nu, \mathbf{p}) \in \mathbb{R}^{3n_u} \times \mathbf{K}_\omega(\mathscr{F}\mathbf{g}) \times \mathbb{R}^{n_s} \times \mathbb{R}^{n_p} \text{ such that} \\ &\mathbf{A}\mathbf{u} - \mathbf{T}_1^T\boldsymbol{\lambda}_{\tau_1} - \mathbf{T}_2^T\boldsymbol{\lambda}_{\tau_2} - \mathbf{N}^T\boldsymbol{\lambda}_\nu - \mathbf{B}^T\mathbf{p} - \mathbf{b} = \mathbf{0} \\ &\mathbf{B}\mathbf{u} + \mathbf{E}\mathbf{p} - \mathbf{c} = \mathbf{0} \\ &\mathbf{N}\mathbf{u} = \mathbf{0} \\ &(\mathbf{T}_1^T(\boldsymbol{\mu}_1 + \boldsymbol{\lambda}_{\tau_1}) + \mathbf{T}_2^T(\boldsymbol{\mu}_2 + \boldsymbol{\lambda}_{\tau_2})) \cdot \mathbf{u} \le 0 \quad \forall \boldsymbol{\mu} = (\boldsymbol{\mu}_1, \boldsymbol{\mu}_2) \in \mathbf{K}_\omega(\mathscr{F}\mathbf{g}) \end{aligned}\right\} \tag{4.7}$$

where $\mathbf{A} \in \mathbb{R}^{3n_u \times 3n_u}$ is the symmetric, positive definite diffusion matrix, $\mathbf{B} \in \mathbb{R}^{n_p \times 3n_u}$ is the full row rank divergence matrix, $\mathbf{b} \in \mathbb{R}^{3n_u}$ is the discrete source term, and the symmetric, positive semidefinite matrix $\mathbf{E} \in \mathbb{R}^{n_p \times n_p}$ and the vector $\mathbf{c} \in \mathbb{R}^{n_p}$ arise from the elimination of the bubble components of $\mathbf{u}$ (on the element level). The matrices are assembled by vectorized codes proposed in [26] for the Laplace operator and modified in [3] for the operator

$-2\,\mathrm{div}\,\mathbb{D}$ used in (2.1); see also free available codes [27]. Let us recall that $\boldsymbol{\lambda}_{\tau_j}$, $j = 1, 2$, $\boldsymbol{\lambda}_\nu$ are the algebraic shear and normal stresses, respectively. Dividing the ith components of these vectors by ω_i for all $i \in \mathcal{N}$ we obtain their physical counterparts $\mathbf{l}_\tau, \mathbf{l}_\nu$ which represent the shear and normal stresses on S at the slip nodes.

If (4.7) represents the kth iteration in the method of successive approximations, the slip bound vector $\mathbf{g}$ in (4.7) is given by the vector of the discrete normal stress on S from the $(k-1)$-th iteration, i.e. $\mathbf{g} = \mathbf{l}_\nu^{(k-1)}$. Hence $\mathbf{K}_\omega(\mathscr{F}\mathbf{l}_\nu^{(k-1)}) = \mathbf{K}(\mathscr{F}\boldsymbol{\lambda}_\nu^{(k-1)})$ and the kth iteration reads as follows:

$$\left.\begin{array}{rll} \text{Find } (\mathbf{u}, (\boldsymbol{\lambda}_{\tau_1}, \boldsymbol{\lambda}_{\tau_2}), \boldsymbol{\lambda}_\nu, \mathbf{p}) \in \mathbb{R}^{3n_u} \times \mathbf{K}(\mathscr{F}\boldsymbol{\lambda}_\nu^{(k-1)}) \times \mathbb{R}^{n_s} \times \mathbb{R}^{n_p} \text{ such that} & & \\ \mathbf{A}\mathbf{u} - \mathbf{T}_1^T\boldsymbol{\lambda}_{\tau_1} - \mathbf{T}_2^T\boldsymbol{\lambda}_{\tau_2} - \mathbf{N}^T\boldsymbol{\lambda}_\nu - \mathbf{B}^T\mathbf{p} - \mathbf{b} & = \mathbf{0} & \\ \mathbf{B}\mathbf{u} + \mathbf{E}\mathbf{p} - \mathbf{c} & = \mathbf{0} & \\ \mathbf{N}\mathbf{u} & = \mathbf{0} & \\ (\mathbf{T}_1^T(\boldsymbol{\mu}_1 + \boldsymbol{\lambda}_{\tau_1}) + \mathbf{T}_2^T(\boldsymbol{\mu}_2 + \boldsymbol{\lambda}_{\tau_2}))\cdot\mathbf{u} & \le 0 \quad \forall \boldsymbol{\mu} = (\boldsymbol{\mu}_1, \boldsymbol{\mu}_2) \in \mathbf{K}(\mathscr{F}\boldsymbol{\lambda}_\nu^{(k-1)}) & \end{array}\right\} \tag{4.8}$$

Replacing $\boldsymbol{\lambda}_\nu^{(k-1)}$ by $\boldsymbol{\lambda}_\nu$ in (4.8) we obtain the algebraic formulation of $(\mathscr{P})_{\mathrm{IVF}}$.

Remark 4.1. The analogue of Remark 2.2 remains true also for the solution $(\mathbf{u}, (\boldsymbol{\lambda}_{\tau_1}, \boldsymbol{\lambda}_{\tau_2}), \boldsymbol{\lambda}_\nu, \mathbf{p})$ to the discretized problem $(\mathscr{P})_{\mathrm{IVF}}$. If $(\boldsymbol{\lambda}_\nu)_i \neq 0$ and $\|((\boldsymbol{\lambda}_{\tau_1})_i, (\boldsymbol{\lambda}_{\tau_2})_i)\| < \mathscr{F}|(\boldsymbol{\lambda}_\nu)_i|$ for all $i \in \mathcal{N}$ then $(\mathbf{u})_i = 0$ for all $i \in \mathcal{N}$. Also the remaining statements of Remark 2.2 hold true in the discrete case.

5. Algorithms

The aim of this section is to present algorithms for solving the problem with the Coulomb stick–slip boundary conditions. To this end we use the semi-smooth Newton method. Under appropriate boundedness assumptions on the inverse of generalized Jacobian matrices convergence of the method is superlinear provided that the initial approximation is close to the solution [14,24]. We will use two strategies. The first one combines the method of successive approximations with the Newton iterations applied to the solution of the Stokes problem with the Tresca slip conditions. In the second strategy the semi-smooth Newton method is applied directly to the algebraic formulation of the problem with the Coulomb slip conditions. In both cases we formulate the respective stick–slip law as nonsmooth equations using the projection on the circle in $\mathbb{R}^2$.

Remark 5.1. Unlike the previous section we consider all dual variables with the opposite sign, i.e. $\boldsymbol{\lambda}_{\tau_1} := -\boldsymbol{\lambda}_{\tau_1}$, $\boldsymbol{\lambda}_{\tau_2} := -\boldsymbol{\lambda}_{\tau_2}$, $\boldsymbol{\lambda}_\nu := -\boldsymbol{\lambda}_\nu$, and $\mathbf{p} := -\mathbf{p}$. The reason is that the Schur complements introduced below are given by generalized saddle-point matrices, where this convention leads to standard notation. Moreover, all vectors will be considered in the column form.

Let $C(r) = \{\mathbf{x} \in \mathbb{R}^2 : \|\mathbf{x}\| \le r\}$ denote the circle of radius $r \ge 0$ and $\mathbf{P}(\cdot, r) : \mathbb{R}^2 \to C(r)$ be the projection defined by:

$$\mathbf{P}(\mathbf{x}; r) = \begin{cases} \mathbf{x} & \text{for } \|\mathbf{x}\| \le r, \\ \dfrac{r}{\|\mathbf{x}\|}\mathbf{x} & \text{for } \|\mathbf{x}\| > r. \end{cases}$$

It is easy to show that the Tresca and Coulomb stick–slip laws in $(4.7)_5$ and $(4.8)_5$ are equivalent to

$$^i\boldsymbol{\lambda}_\tau = \mathbf{P}(^i\boldsymbol{\lambda}_\tau + \rho\ ^i\mathbf{u}_\tau; \mathscr{F}g_i), \quad i \in \mathcal{N}, \tag{5.1}$$

and

$$^i\boldsymbol{\lambda}_\tau = \mathbf{P}(^i\boldsymbol{\lambda}_\tau + \rho\ ^i\mathbf{u}_\tau; \mathscr{F}|(\boldsymbol{\lambda}_\nu)_i|), \quad i \in \mathcal{N}, \tag{5.2}$$

respectively. Recall that $^i\boldsymbol{\lambda}_\tau = ((\boldsymbol{\lambda}_{\tau_1})_i, (\boldsymbol{\lambda}_{\tau_2})_i)$, $^i\mathbf{u}_\tau = ((\mathbf{T}_1\mathbf{u})_i, (\mathbf{T}_2\mathbf{u})_i)$, and $\rho > 0$ is an arbitrary but fixed parameter.

The semi-smooth Newton method needs the generalized Jacobian matrix $\partial_{\mathbf{x}}\mathbf{P} : \mathbb{R}^2 \to \mathbb{R}^{2\times 2}$ to the solved system. It will be defined by:

$$\partial_{\mathbf{x}}\mathbf{P}(\mathbf{x}; r) = \begin{cases} \mathbf{I} & \text{for } \|\mathbf{x}\| \le r, \\ \dfrac{r}{\|\mathbf{x}\|}\left(\mathbf{I} - \dfrac{1}{\|\mathbf{x}\|^2}\mathbf{x}\mathbf{x}^T\right) & \text{for } \|\mathbf{x}\| > r. \end{cases} \tag{5.3}$$

In the case of the Coulomb law we will also need the generalized derivative of $\mathbf{P}(\mathbf{x}; \mathscr{F}|y|)$ with respect to $y \in \mathbb{R}$:

$$\partial_y \mathbf{P}(\mathbf{x}; \mathscr{F}|y|) = \begin{cases} \mathbf{0} & \text{for } \|\mathbf{x}\| \le \mathscr{F}|y|, \\ \dfrac{\mathscr{F}\,\operatorname{sgn} y}{\|\mathbf{x}\|}\mathbf{x} & \text{for } \|\mathbf{x}\| > \mathscr{F}|y|. \end{cases} \tag{5.4}$$

Note that the projection on the circle in 3D is replaced by the projection on a finite interval in 2D. This simplifies considerably the structure of the respective Jacobian matrices. Moreover, it leads to the symmetric, positive definite Schur complements for the Tresca slip conditions. Thus the conjugate gradient method (CGM) can be used as the natural inner solver [20,21]. The 3D case is more involved as it will be seen from the next subsections.

5.1. Method of successive approximations

In this subsection we describe in more details how to implement the method of successive approximations (4.8). First of all we show how to solve subproblems (4.7) by the semi-smooth Newton method. Introducing the new (artificial) variables $\mathbf{s}_\tau = (\mathbf{s}_{\tau_1}, \mathbf{s}_{\tau_2}) \in \mathbb{R}^{n_s} \times \mathbb{R}^{n_s}$, ${}^i\mathbf{s}_\tau = (({}^i\mathbf{s}_{\tau_1})_i, ({}^i\mathbf{s}_{\tau_2})_i) \in \mathbb{R}^2$ by

$${}^i\mathbf{s}_\tau = {}^i\boldsymbol{\lambda}_\tau + \rho\, {}^i\mathbf{u}_\tau, \quad i \in \mathscr{N}$$

and using them in (5.1) we can rewrite (5.1) as follows:

$${}^i\mathbf{u}_\tau - \rho^{-1}({}^i\mathbf{s}_\tau - \mathbf{P}({}^i\mathbf{s}_\tau; \mathscr{F} g_i)) = \mathbf{0}, \quad i \in \mathscr{N}.$$

Remark 5.2. The reason for introducing the vector $\mathbf{s}_\tau$ is to symmetrize Jacobian matrix and its positive definite Schur complement. It was noticed already for contact problems of linear elasticity that the projection on the circle results in non-symmetric matrices. In [29] the contact problem was symmetrized by omitting the non-symmetric block without influence on the computed solution. This symmetrization is technically difficult in the present case. Here we are inspired by [19] devoted to the Stokes problem with the Navier–Tresca slip law, where $\mathbf{s}_\tau$ plays the role of the discrete shear stress leading to the Schur complement that is unconditionally positive definite and symmetric. But for the pure Tresca law, the variable $\mathbf{s}_\tau$ exhibits an artificial character and it results in symmetric, positive definite Schur complement only if the parameter $\rho > 0$ is sufficiently small.

The whole system (4.7) can be equivalently written as the nonsmooth equation:

$$\mathbf{G}(\mathbf{y}) = \mathbf{0} \tag{5.5}$$

with $\mathbf{G} : \mathbb{R}^{3n_u+3n_s+n_p} \to \mathbb{R}^{3n_u+3n_s+n_p}$ defined at $\mathbf{y} = (\mathbf{u}^T, \mathbf{s}_{\tau_1}^T, \mathbf{s}_{\tau_1}^T, \boldsymbol{\lambda}_\nu^T, \mathbf{p}^T)^T$ by

$$\mathbf{G}(\mathbf{y}) := \begin{pmatrix} \mathbf{A}_\rho \mathbf{u} + \mathbf{T}_1^T \mathbf{s}_{\tau_1} + \mathbf{T}_2^T \mathbf{s}_{\tau_2} + \mathbf{N}^T \boldsymbol{\lambda}_\nu + \mathbf{B}^\top \mathbf{p} - \mathbf{b} \\ \mathbf{T}_1 \mathbf{u} - \rho^{-1}(\mathbf{s}_{\tau_1} - \boldsymbol{\Pi}_1(\mathbf{s}_\tau)) \\ \mathbf{T}_2 \mathbf{u} - \rho^{-1}(\mathbf{s}_{\tau_2} - \boldsymbol{\Pi}_2(\mathbf{s}_\tau)) \\ \mathbf{N}\mathbf{u} \\ \mathbf{B}\mathbf{u} - \mathbf{E}\mathbf{p} - \mathbf{c} \end{pmatrix},$$

where $\mathbf{A}_\rho = \mathbf{A} - \rho(\mathbf{T}_1^T\mathbf{T}_1 + \mathbf{T}_2^T\mathbf{T}_2)$, $\boldsymbol{\Pi}_j(\mathbf{s}_\tau) = (P_j({}^1\mathbf{s}_\tau; \mathscr{F} g_1), \dots, P_j({}^{n_s}\mathbf{s}_\tau; \mathscr{F} g_{n_s}))^T \in \mathbb{R}^{n_s}$, and P_j stands for the jth component of $\mathbf{P}$, $j = 1, 2$. Note that $\mathbf{A}_\rho$ is positive definite only if $\rho > 0$ is sufficiently small.

Eq. (5.5) will be solved by the Newton iterations:

$$\mathbf{J}_G(\mathbf{y}^{(k)})\mathbf{y}^{(k+1)} = \mathbf{J}_G(\mathbf{y}^{(k)})\mathbf{y}^{(k)} - \mathbf{G}(\mathbf{y}^{(k)}), \quad k = 0, 1, \dots, \tag{5.6}$$

where $\mathbf{J}_G(\mathbf{y})$ is an arbitrary non-singular generalized Jacobian matrix of $\mathbf{G}$ at $\mathbf{y}$ and $\mathbf{y}^{(0)}$ is an initial approximation. We will use the active/inactive set implementation of (5.6). Let $\mathscr{A}, \mathscr{I} \subseteq \mathscr{N}$ be the *active*, and *inactive* set at $\mathbf{y}$, respectively:

$$\mathscr{A} := \mathscr{A}(\mathbf{y}) = \{i \in \mathscr{N} : \ \|{}^i\mathbf{s}_\tau\| \le \mathscr{F} g_i\}, \quad \mathscr{I} := \mathscr{I}(\mathbf{y}) = \mathscr{N} \setminus \mathscr{A}$$

and let $\mathbf{I}_{\mathscr{A}}, \mathbf{I}_{\mathscr{I}} \in \mathbb{R}^{n_s \times n_s}$ be the indicator matrices of $\mathscr{A}$ and $\mathscr{I}$, respectively. Using them in the definition of $\mathbf{G}$ we have:

$$\mathbf{G}(\mathbf{y}) = \begin{pmatrix} \mathbf{A}_\rho \mathbf{u} + \mathbf{T}_1^T \mathbf{s}_{\tau_1} + \mathbf{T}_2^T \mathbf{s}_{\tau_2} + \mathbf{N}^T \boldsymbol{\lambda}_\nu + \mathbf{B}^\top \mathbf{p} - \mathbf{b} \\ \mathbf{T}_1 \mathbf{u} - \rho^{-1}(\mathbf{I}_{\mathscr{I}} - \mathbf{D}_{\mathscr{F}\mathbf{g}/\|\mathbf{s}_\tau\|})\mathbf{s}_{\tau_1} \\ \mathbf{T}_2 \mathbf{u} - \rho^{-1}(\mathbf{I}_{\mathscr{I}} - \mathbf{D}_{\mathscr{F}\mathbf{g}/\|\mathbf{s}_\tau\|})\mathbf{s}_{\tau_2} \\ \mathbf{N}\mathbf{u} \\ \mathbf{B}\mathbf{u} - \mathbf{E}\mathbf{p} - \mathbf{c} \end{pmatrix},$$

where

$$\mathbf{D}_{\mathscr{F}\mathbf{g}/\|\mathbf{s}_\tau\|} = diag(d_1, \ldots, d_{n_s}),\ d_i = \mathscr{F} g_i / \|^i \mathbf{s}_\tau\| \text{ if } i \in \mathscr{I},\ d_i = 0 \text{ if } i \notin \mathscr{I}.$$

Standard differentiation rules and (5.3) yield:

$$\mathbf{J}_G(\mathbf{y}) = \left(\begin{array}{c|cccc} \mathbf{A}_\rho & \mathbf{T}_1^T & \mathbf{T}_2^T & \mathbf{N}^T & \mathbf{B}^T \\ \hline \mathbf{T}_1 & -\mathbf{D}_{11} & -\mathbf{D}_{12} & \mathbf{0} & \mathbf{0} \\ \mathbf{T}_2 & -\mathbf{D}_{12} & -\mathbf{D}_{22} & \mathbf{0} & \mathbf{0} \\ \mathbf{N} & \mathbf{0} & \mathbf{0} & \mathbf{0} & \mathbf{0} \\ \mathbf{B} & \mathbf{0} & \mathbf{0} & \mathbf{0} & -\mathbf{E} \end{array}\right), \tag{5.7}$$

where

$$\mathbf{D}_{jj} = \rho^{-1}(\mathbf{I}_{\mathscr{I}} - \mathbf{D}_{\mathscr{F}\mathbf{g}/\|\mathbf{s}_\tau\|}(\mathbf{I}_{\mathscr{I}} - \mathbf{D}_{1/\|\mathbf{s}_\tau\|^2}\mathbf{D}^2_{\mathbf{s}_{\tau_j}})),\ \ j = 1, 2,$$
$$\mathbf{D}_{12} = \rho^{-1}\mathbf{D}_{\mathscr{F}\mathbf{g}/\|\mathbf{s}_\tau\|}\mathbf{D}_{1/\|\mathbf{s}_\tau\|^2}\mathbf{D}_{\mathbf{s}_{\tau_1}}\mathbf{D}_{\mathbf{s}_{\tau_2}},$$
$$\mathbf{D}_{1/\|\mathbf{s}_\tau\|^2} = diag\ (d_1, \ldots, d_{n_s}),\ d_i = 1/\|^i \mathbf{s}_\tau\|^2 \text{ if } i \in \mathscr{I},\ d_i = 0 \text{ if } i \notin \mathscr{I},$$
$$\mathbf{D}_{\mathbf{s}_{\tau_j}} = diag\ (\mathbf{s}_{\tau_j}),\ \ j = 1, 2.$$

To solve the linear systems in (5.6), we use the Schur complement $\mathbf{S}_\rho$ to (1,1)-block in (5.7) defined by:

$$\mathbf{S}_\rho = \mathbf{F}_\rho + \mathbf{D}, \tag{5.8}$$

where $\mathbf{F}_\rho = \mathbf{C}\mathbf{A}_\rho^{-1}\mathbf{C}^T$ with $\mathbf{C} = (\mathbf{T}_1^T, \mathbf{T}_2^T, \mathbf{N}^T, \mathbf{B}^T)^\top$ and $\mathbf{D} = diag\left(\begin{pmatrix} \mathbf{D}_{11} & \mathbf{D}_{12} \\ \mathbf{D}_{12} & \mathbf{D}_{22} \end{pmatrix}, \mathbf{0}, \mathbf{E}\right)$. The right hand-sides of the Schur complement linear systems are:

$$\mathbf{d} = \mathbf{C}\mathbf{A}_\rho^{-1}\mathbf{b} - (\mathbf{h}_1^T, \mathbf{h}_2^T, \mathbf{0}^T, \mathbf{c}^T)^T, \tag{5.9}$$

where

$$\mathbf{h}_1 = -\rho^{-1}\mathbf{D}_{\mathscr{F}\mathbf{g}/\|\mathbf{s}_\tau\|}\mathbf{D}_{1/\|\mathbf{s}_\tau\|^2}(\mathbf{D}^2_{\mathbf{s}_{\tau_1}}\mathbf{s}_{\tau_1} + \mathbf{D}_{\mathbf{s}_{\tau_1}}\mathbf{D}_{\mathbf{s}_{\tau_2}}\mathbf{s}_{\tau_2}),$$
$$\mathbf{h}_2 = -\rho^{-1}\mathbf{D}_{\mathscr{F}\mathbf{g}/\|\mathbf{s}_\tau\|}\mathbf{D}_{1/\|\mathbf{s}_\tau\|^2}(\mathbf{D}_{\mathbf{s}_{\tau_1}}\mathbf{D}_{\mathbf{s}_{\tau_2}}\mathbf{s}_{\tau_1} + \mathbf{D}^2_{\mathbf{s}_{\tau_2}}\mathbf{s}_{\tau_2}).$$

We arrive at the implementation of (5.6), in which the iterations are performed with the last four components of $\mathbf{y}$ assembled in the vector $\boldsymbol{\lambda} = (\mathbf{s}_{\tau_1}^T, \mathbf{s}_{\tau_2}^T, \boldsymbol{\lambda}_\nu^T, \mathbf{p}^T)^T \in \mathbb{R}^{3n_s+n_p}$:

ALGORITHM SSN_TRESCA [Given $\boldsymbol{\lambda}^{(0)} \in \mathbb{R}^{3n_s+n_p}$, $\mathbf{g} \in \mathbb{R}^{n_s}_+$, $\rho > 0$, $tol > 0$.] Set $k := 0$.

(i) Assemble the active/inactive sets $\mathscr{A}$ and $\mathscr{I}$ at $\boldsymbol{\lambda}^{(k)}$, the matrix $\mathbf{D}$ and the vectors $\mathbf{h}_1, \mathbf{h}_2$ to build $\mathbf{S}_\rho$ and $\mathbf{d}$ by (5.8) and (5.9), respectively.

(ii) Using CGM solve the linear system:

$$\mathbf{S}_\rho \boldsymbol{\lambda}^{(k+1)} = \mathbf{d}. \tag{5.10}$$

(iii) Return $\boldsymbol{\lambda}_{sol} = \boldsymbol{\lambda}^{(k+1)}$, if $\|\boldsymbol{\lambda}^{(k+1)} - \boldsymbol{\lambda}^{(k)}\| / \|\boldsymbol{\lambda}^{(k+1)}\| \le tol$, else set $k := k + 1$ and go to step *(i)*.

From the definition we see that the matrix $\mathbf{D}$ is symmetric, positive semidefinite and consequently $\mathbf{S}_\rho$ is symmetric, positive definite for sufficiently small ρ. It is well-known that CGM is not efficient, if the spectral condition number of the system matrix is large. In order to improve conditioning of (5.10), we use the diagonal preconditioner:

$$\mathbf{P}_{\mathbf{S}_\rho} := diag\, \mathbf{F}_\rho + diag\, (\mathbf{D}_{11}, \mathbf{D}_{22}, \mathbf{0}, diag\, \mathbf{E})\,. \tag{5.11}$$

Let us note that the following result analogous to [28] can be established:

$$cond\,(\mathbf{P}_{\mathbf{S}_\rho}^{-1}\mathbf{S}_\rho) \le cond\,(diag\,\mathbf{F}_\rho)cond\,(\mathbf{F}_\rho).$$

Finally note that an appropriate values of $\rho > 0$ guaranteeing positive definiteness of $\mathbf{A}_\rho$ are computed experimentally using the backtracking procedure so that the Cholesky factorization of $\mathbf{A}_\rho$ is executed in Matlab.

To realize the method of successive approximations (4.8) we propose its inexact implementation with an adaptive precision control.

ALGORITHM MSA [Given $\boldsymbol{\lambda}^{(0)} \in \mathbb{R}^{3n_s+n_p}$, $\mathbf{g}^{(0)} := |\boldsymbol{\lambda}_\nu^{(0)}| \in \mathbb{R}^{n_s}_+$, $\rho > 0$, $\varepsilon > 0$, $0 < r_{tol}, c_{fact} < 1$.] Set $l := 0$ and $tol^{(0)} := r_{tol}/c_{fact}$.

(j) Compute $\boldsymbol{\lambda}^{(l+1)} = \text{SSN\_TRESCA}[\boldsymbol{\lambda}^{(l)}, \mathbf{g}^{(l)} := |\boldsymbol{\lambda}_\nu^{(l)}|, \rho, tol^{(l)}]$.

(jj) Compute $err^{(l)} := \|\boldsymbol{\lambda}^{(l+1)} - \boldsymbol{\lambda}^{(l)}\|/\|\boldsymbol{\lambda}^{(l+1)}\|$.

(jjj) If $err^{(l)} \le \varepsilon$, stop, else set $l := l + 1$, $tol^{(l)} := \min\{r_{tol} \times err^{(l-1)}, c_{fact} \times tol^{(l-1)}\}$ and go to step *(j)*.

(jv) Return $\boldsymbol{\lambda} = \boldsymbol{\lambda}^{(l+1)}$ and $\mathbf{u} = \mathbf{A}^{-1}(\mathbf{b} - \mathbf{C}^T\boldsymbol{\lambda})$.

Recall that the absolute value of vectors is understood componentwisely. Since MSA is a two-level iteration process we used an adaptive precision control in which the precision of the outer and inner loop are linked. The inner ALGORITHM SSN_TRESCA used in step *(j)* is initialized and terminated adaptively. It respects the precision control $err^{(l-1)}$ achieved in the current step sharpened by the parameter r_{tol}. If the progress is not sufficient, the terminating tolerance $tol^{(l-1)}$ is also sharpened using the parameter c_{fact}. These parameters are chosen in advance.

5.2. Direct solution of the coulomb problem

In this subsection we solve the problem with the Coulomb stick–slip boundary conditions directly by the semi-smooth Newton method. The respective nonsmooth equation is obtained from (4.8) and (5.2) replacing g_i by $|(\boldsymbol{\lambda}_\nu)_i|$, $i \in \mathcal{N}$ and it reads as follows:

$$\mathbf{H}(\mathbf{y}) = \mathbf{0}, \tag{5.12}$$

where $\mathbf{H} : \mathbb{R}^{3n_u+3n_s+n_p} \to \mathbb{R}^{3n_u+3n_s+n_p}$ is defined at $\mathbf{y} = (\mathbf{u}^T, \boldsymbol{\lambda}_{\tau_1}^T, \boldsymbol{\lambda}_{\tau_1}^T, \boldsymbol{\lambda}_\nu^T, \mathbf{p}^T)^T$ by

$$\mathbf{H}(\mathbf{y}) := \begin{pmatrix} \mathbf{A}\mathbf{u} + \mathbf{T}_1^T\boldsymbol{\lambda}_{\tau_1} + \mathbf{T}_2^T\boldsymbol{\lambda}_{\tau_2} + \mathbf{N}^T\boldsymbol{\lambda}_\nu + \mathbf{B}^T\mathbf{p} - \mathbf{b} \\ \boldsymbol{\Pi}_1(\mathbf{u}, \boldsymbol{\lambda}_{\tau_1}, \boldsymbol{\lambda}_{\tau_2}, \boldsymbol{\lambda}_\nu) - \boldsymbol{\lambda}_{\tau_1} \\ \boldsymbol{\Pi}_2(\mathbf{u}, \boldsymbol{\lambda}_{\tau_1}, \boldsymbol{\lambda}_{\tau_2}, \boldsymbol{\lambda}_\nu) - \boldsymbol{\lambda}_{\tau_2} \\ \mathbf{N}\mathbf{u} \\ \mathbf{B}\mathbf{u} - \mathbf{E}\mathbf{p} - \mathbf{c} \end{pmatrix}$$

with $\boldsymbol{\Pi}_j(\mathbf{u}, \boldsymbol{\lambda}_{\tau_1}, \boldsymbol{\lambda}_{\tau_2}, \boldsymbol{\lambda}_\nu) = (P_j({}^1\boldsymbol{\lambda}_\tau + \rho\,{}^1\mathbf{u}_\tau; \mathscr{F}|(\boldsymbol{\lambda}_\nu)_1|), \dots, P_j({}^{n_s}\boldsymbol{\lambda}_\tau + \rho\,{}^{n_s}\mathbf{u}_\tau; \mathscr{F}|(\boldsymbol{\lambda}_\nu)_{n_s}|))^T$ and P_j standing for the jth component of $\mathbf{P}$, $j = 1, 2$.

Eq. (5.12) will be solved by the Newton iterations (5.6) (with $\mathbf{G}$ replaced by $\mathbf{H}$). Now the *active*, and *inactive* sets at $\mathbf{y}$ are defined by:

$$\mathscr{A} := \mathscr{A}(\mathbf{y}) = \{i \in \mathcal{N} : \|{}^i\boldsymbol{\lambda}_\tau + \rho\,{}^i\mathbf{u}_\tau\| \le \mathscr{F}|(\boldsymbol{\lambda}_\nu)_i|\}, \quad \mathscr{I} := \mathscr{I}(\mathbf{y}) = \mathcal{N} \setminus \mathscr{A},$$

respectively. Let $\mathbf{I}_\mathscr{A}, \mathbf{I}_\mathscr{I} \in \mathbb{R}^{n_s \times n_s}$ be the indicator matrices for $\mathscr{A}$ and $\mathscr{I}$, respectively. Using them in the definition of $\mathbf{H}$ we see that

$$\mathbf{H}(\mathbf{y}) = \begin{pmatrix} \mathbf{A}\mathbf{u} + \mathbf{T}_1^T\boldsymbol{\lambda}_{\tau_1} + \mathbf{T}_2^T\boldsymbol{\lambda}_{\tau_2} + \mathbf{N}^T\boldsymbol{\lambda}_\nu + \mathbf{B}^T\mathbf{p} - \mathbf{b} \\ \rho(\mathbf{I}_\mathscr{A} + \mathbf{D}_\mathscr{F})\mathbf{T}_1\mathbf{u} - (\mathbf{I}_\mathscr{I} - \mathbf{D}_\mathscr{F})\boldsymbol{\lambda}_{\tau_1} \\ \rho(\mathbf{I}_\mathscr{A} + \mathbf{D}_\mathscr{F})\mathbf{T}_2\mathbf{u} - (\mathbf{I}_\mathscr{I} - \mathbf{D}_\mathscr{F})\boldsymbol{\lambda}_{\tau_2} \\ \mathbf{N}\mathbf{u} \\ \mathbf{B}\mathbf{u} - \mathbf{E}\mathbf{p} - \mathbf{c} \end{pmatrix},$$

where

$$\mathbf{D}_\mathscr{F} = diag\,(d_1, \dots, d_{n_s}),\ d_i = \mathscr{F}|(\boldsymbol{\lambda}_\nu)_i|/\|{}^i\boldsymbol{\lambda}_\tau + \rho\,{}^i\mathbf{u}_\tau\| \text{ if } i \in \mathscr{I},\ d_i = 0 \text{ if } i \notin \mathscr{I}.$$

Standard differentiation rules, (5.3), (5.4), and the fact that $\mathbf{I}_{\mathscr{J}}\mathbf{D}_{\mathscr{F}} = \mathbf{D}_{\mathscr{F}}$ yield:

$$\mathbf{J}_H(\mathbf{y}) = \left(\begin{array}{c|cccc} \mathbf{A} & \mathbf{T}_1^T & \mathbf{T}_2^T & \mathbf{N}^T & \mathbf{B}^T \\ \hline \mathbf{D}_{11} & -\mathbf{D}_{12} & -\mathbf{D}_{13} & -\mathbf{D}_{14} & \mathbf{0} \\ \mathbf{D}_{21} & -\mathbf{D}_{22} & -\mathbf{D}_{23} & -\mathbf{D}_{24} & \mathbf{0} \\ \mathbf{N} & \mathbf{0} & \mathbf{0} & \mathbf{0} & \mathbf{0} \\ \mathbf{B} & \mathbf{0} & \mathbf{0} & \mathbf{0} & -\mathbf{E} \end{array}\right), \tag{5.13}$$

where

$$\begin{aligned} &\mathbf{D}_{11} = \rho(\mathbf{I}_{\mathscr{A}} + \mathbf{D}_{\mathscr{F}})\mathbf{T}_1 - \rho\mathbf{D}_{\mathscr{F}}(\mathbf{D}_1^2\mathbf{T}_1 + \mathbf{D}_1\mathbf{D}_2\mathbf{T}_2), \\ &\mathbf{D}_{21} = \rho(\mathbf{I}_{\mathscr{A}} + \mathbf{D}_{\mathscr{F}})\mathbf{T}_2 - \rho\mathbf{D}_{\mathscr{F}}(\mathbf{D}_1\mathbf{D}_2\mathbf{T}_1 + \mathbf{D}_2^2\mathbf{T}_2), \\ &\mathbf{D}_{12} = -\mathbf{D}_{\mathscr{F}} + \mathbf{D}_{\mathscr{F}}\mathbf{D}_1^2 + \mathbf{I}_{\mathscr{J}},\ \ \mathbf{D}_{23} = -\mathbf{D}_{\mathscr{F}} + \mathbf{D}_{\mathscr{F}}\mathbf{D}_2^2 + \mathbf{I}_{\mathscr{J}}, \\ &\mathbf{D}_{22} = \mathbf{D}_{13} = \mathbf{D}_{\mathscr{F}}\mathbf{D}_1\mathbf{D}_2, \\ &\mathbf{D}_{14} = -\mathbf{D}_{\mathscr{F}\boldsymbol{\lambda}_v}\mathbf{D}_1,\ \ \mathbf{D}_{24} = -\mathbf{D}_{\mathscr{F}\boldsymbol{\lambda}_v}\mathbf{D}_2 \end{aligned}$$

and

$$\begin{aligned} &\mathbf{D}_j = diag\ (d_1, \dots, d_{n_s}),\ \ d_i = ((\boldsymbol{\lambda}_{\tau_j})_i + \rho(\mathbf{u}_{\tau_j})_i)/\|{}^i\boldsymbol{\lambda}_\tau + \rho\,{}^i\mathbf{u}_\tau\| \text{ if } i \in \mathscr{I},\ \ d_i = 0 \text{ if } i \notin \mathscr{I} \text{ for } j = 1, 2, \\ &\mathbf{D}_{\mathscr{F}\boldsymbol{\lambda}_v} = diag\ (\mathscr{F}\ \mathrm{sgn}(\boldsymbol{\lambda}_v)_1, \dots, \mathscr{F}\ \mathrm{sgn}(\boldsymbol{\lambda}_v)_{n_s}). \end{aligned}$$

To solve the linear systems (5.6) with $\mathbf{J}_H$ in place of $\mathbf{J}_G$, we use the Schur complement $\mathbf{S}$ to (1,1)-block in (5.13) defined by:

$$\mathbf{S} = \mathbf{F} + \mathbf{D} \tag{5.14}$$

with $\mathbf{F} = \mathbf{C}_L\mathbf{A}^{-1}\mathbf{C}_U^T$, where $\mathbf{C}_L$, $\mathbf{C}_U$ are the lower and upper off-diagonal blocks in (5.13), respectively, and

$$\mathbf{D} = \left(\begin{array}{cccc} \mathbf{D}_{12} & \mathbf{D}_{13} & \mathbf{D}_{14} & \mathbf{0} \\ \mathbf{D}_{22} & \mathbf{D}_{23} & \mathbf{D}_{24} & \mathbf{0} \\ \mathbf{0} & \mathbf{0} & \mathbf{0} & \mathbf{0} \\ \mathbf{0} & \mathbf{0} & \mathbf{0} & \mathbf{E} \end{array}\right).$$

The right hand-sides of the Schur complement linear systems are:

$$\mathbf{d} = \mathbf{C}_L\mathbf{A}^{-1}\mathbf{b} - (\mathbf{h}_1^T, \mathbf{h}_2^T, \mathbf{0}^T, \mathbf{c}^T)^T, \tag{5.15}$$

where

$$\begin{aligned} \mathbf{h}_1 &= -\rho\mathbf{D}_{\mathscr{F}}(\mathbf{D}_1^2\mathbf{T}_1 + \mathbf{D}_1\mathbf{D}_2\mathbf{T}_2)\mathbf{u} - \mathbf{D}_{\mathscr{F}}\mathbf{D}_1(\mathbf{D}_1\boldsymbol{\lambda}_{\tau_1} + \mathbf{D}_2\boldsymbol{\lambda}_{\tau_2}) + \mathbf{D}_{\mathscr{F}\,\mathrm{sgn}(\lambda_v)}\mathbf{D}_1\boldsymbol{\lambda}_v, \\ \mathbf{h}_2 &= -\rho\mathbf{D}_{\mathscr{F}}(\mathbf{D}_1\mathbf{D}_2\mathbf{T}_1 + \mathbf{D}_2^2\mathbf{T}_2)\mathbf{u} - \mathbf{D}_{\mathscr{F}}\mathbf{D}_2(\mathbf{D}_1\boldsymbol{\lambda}_{\tau_1} + \mathbf{D}_2\boldsymbol{\lambda}_{\tau_2}) + \mathbf{D}_{\mathscr{F}\,\mathrm{sgn}(\lambda_v)}\mathbf{D}_2\boldsymbol{\lambda}_v. \end{aligned}$$

We arrive at the following implementation of (5.6), in which the iterations are performed only with the last four components of $\mathbf{y}$ assembled in the vector $\boldsymbol{\lambda} = (\boldsymbol{\lambda}_{\tau_1}^T, \boldsymbol{\lambda}_{\tau_2}^T, \boldsymbol{\lambda}_v^T, \mathbf{p}^T)^T$.

ALGORITHM SSN_COULOMB: [Given $\boldsymbol{\lambda}^{(0)} \in \mathbb{R}^{3n_s+n_p}$, $\varepsilon > 0$, $\rho > 0$.] Set $k := 0$.

(i) Assemble the active/inactive sets $\mathscr{A}$ and $\mathscr{I}$ at $\boldsymbol{\lambda}^{(k)}$, the respective matrix $\mathbf{D}$ and the vectors $\mathbf{h}_1$, $\mathbf{h}_2$ to build $\mathbf{S}$ and $\mathbf{d}$ by (5.14) and (5.15), respectively.

(ii) Using BiCGSTAB solve the linear system:

$$\mathbf{S}\boldsymbol{\lambda}^{(k+1)} = \mathbf{d}. \tag{5.16}$$

(iii) Return $\boldsymbol{\lambda} = \boldsymbol{\lambda}^{(k+1)}$ and $\mathbf{u} = \mathbf{A}^{-1}(\mathbf{b} - \mathbf{C}_U^T\boldsymbol{\lambda})$, if $\|\boldsymbol{\lambda}^{(k+1)} - \boldsymbol{\lambda}^{(k)}\|/\|\boldsymbol{\lambda}^{(k+1)}\| \le \varepsilon$, else set $k := k + 1$ and go to step *(i)*.

In order to improve the performance of BiCGSTAB iterations, we propose the preconditioner analogous to (5.11):

$$\mathbf{P}_S = diag\,\mathbf{F} + diag\,(\mathbf{D}_{12}, \mathbf{D}_{23}, \mathbf{0}, diag\,\mathbf{E})\,.$$

We use the BiCGSTAB implementation presented in [13].

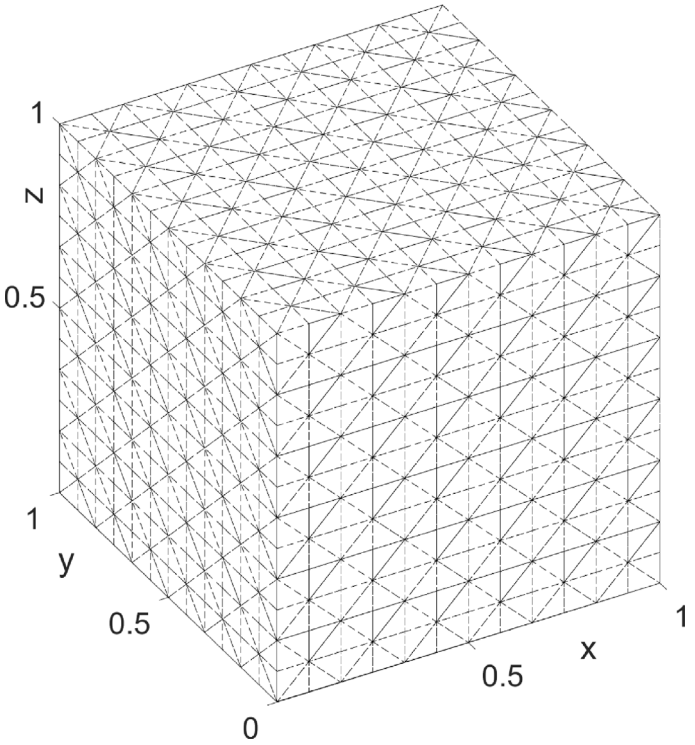

Fig. 1. Cube and 3D mesh.

6. Numerical examples

Recall that the finite element discretization in both examples presented below uses P1+bubble/P1 elements. To guarantee uniqueness of the pressure p (see Remark 2.1) we shall suppose that in addition to Γ and S, there is a non-empty part Γ_N of $\partial\Omega$ with a prescribed value of the stress vector $\boldsymbol{\sigma}$. Finally, both numerical strategies introduced in Section 5 will be used and compared. All computations were done in Matlab R2021a software on supercomputer Karolina [2]. The meshes were generated by iso2mesh software [1].

Example 1 (*Cube*)**.** Let $\Omega = (0,1)^3$ (see Fig. 1). Its boundary $\partial\Omega$ consists of three parts Γ, Γ_N, and S: $\Gamma = \Gamma_{top} \cup \Gamma_{front} \cup \Gamma_{back}$, $\Gamma_N = \Gamma_{left} \cup \Gamma_{right}$, $S = (0,1) \times (0,1) \times \{0\}$, where $\Gamma_{top} = (0,1) \times (0,1) \times \{1\}$, $\Gamma_{front} = \{0\} \times (0,1) \times (0,1)$, $\Gamma_{back} = \{1\} \times (0,1) \times (0,1)$, $\Gamma_{left} = (0,1) \times \{0\} \times (0,1)$, $\Gamma_{right} = (0,1) \times \{1\} \times (0,1)$. Data of problem (2.1) with added $\Gamma_N \neq \emptyset$ are as follows: $\boldsymbol{f} = -2\mu \,\mathrm{div}\, \mathbb{D}(\boldsymbol{u}_{exp}) + \nabla p_{exp}$, $\mu = 1/2$, $\boldsymbol{\sigma}_N = 2\mu\, \mathbb{D}(\boldsymbol{u}_{exp})\, \boldsymbol{\nu} - p_{exp}\, \boldsymbol{\nu}$, and $\mathscr{F} \in \{0.03; 0.5; 1100\}$, where $\boldsymbol{u}_{exp} = (u_{exp,1}, u_{exp,2}, u_{exp,3})$,

$$
\begin{aligned}
u_{exp,1}(x,y,z) &= 4(1-\cos(2\pi x))\sin(2\pi y) z(1-z),\\
u_{exp,2}(x,y,z) &= 4\sin(2\pi x)(\cos(2\pi y)-1) z(1-z),\\
u_{exp,3}(x,y,z) &= 0,\\
p_{exp}(x,y,z) &= 2\pi(-\cos(2\pi x) + 2\cos(2\pi y) - \cos(2\pi z)).
\end{aligned}
$$

It is easy to verify that the couple $(\boldsymbol{u}_{exp}, p_{exp})$ solves the Stokes system in Ω with the no-slip condition on $\Gamma \cup S$ and the Neumann condition with prescribed $\boldsymbol{\sigma}_N$ on Γ_N. Therefore for an appropriate choice of $\mathscr{F}$ it solves also problem (2.1) only with the Dirichlet and Neumann boundary conditions.

Computations were carried out using different meshes characterized by the parameters n_u, n_p, n_c and three values of the slip coefficient $\mathscr{F}$ which enable us to simulate (*a*) pure slip ($\mathscr{F} = 0.03$), (*b*) pure stick ($\mathscr{F} = 1100$), and (*c*) simultaneous stick and slip ($\mathscr{F} = 0.5$) on S. The first experiment was done with the MSA algorithm. The parameters required by this algorithm and its subroutine SSN Tresca are set as follows: $\epsilon = 10^{-5}$, $r_{tol} = 10^{-3}$,

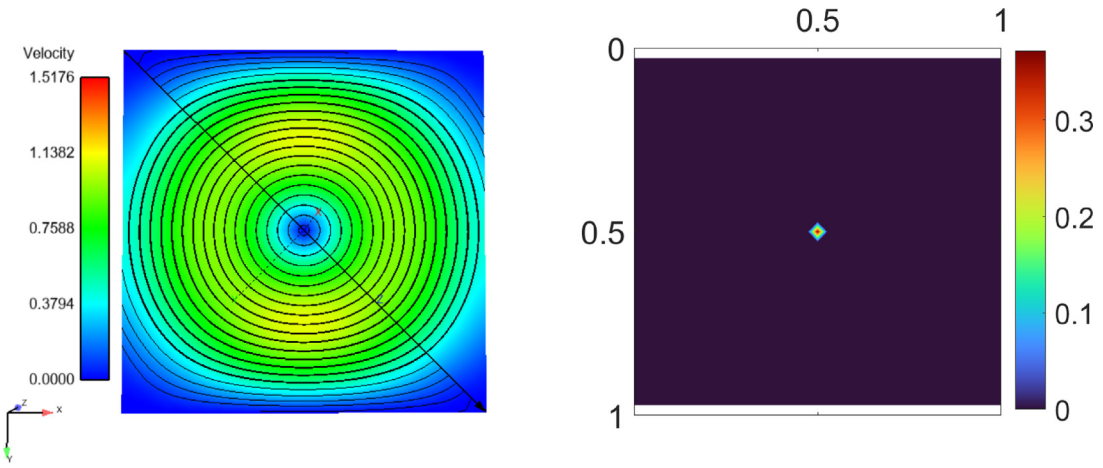

Fig. 2. Tangential velocity field (left), distribution of Ψ (right) on S; $\mathscr{F} = 0.03$.

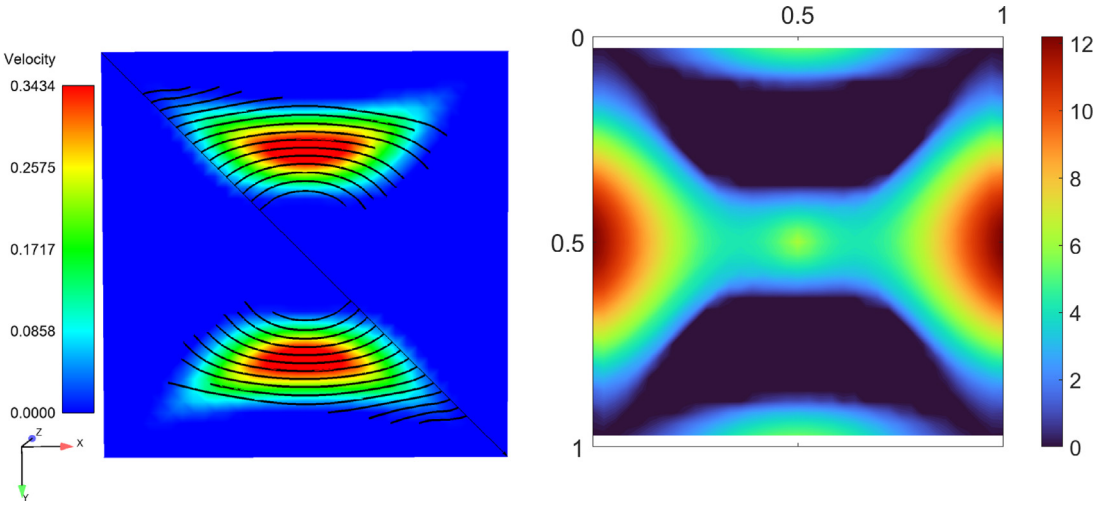

Fig. 3. Tangential velocity field (left), distribution of Ψ (right) on S; $\mathscr{F} = 0.5$.

and $c_{fact} = 0.5$. To show how MSA depends on the initial approximation $\boldsymbol{\lambda}^{(0)}$ we use $\boldsymbol{\lambda}^{(0)} = (\mathbf{0}^T, \mathbf{0}^T, \mathbf{g}^{(0)}, \mathbf{0}^T)^T$, where $\mathbf{g}^{(0)} = (\boldsymbol{\lambda}_v^{(0)})^T$ accordingly to notation introduced in Section 5. We shall consider two cases: (α) $\mathbf{g}^{(0)} = \mathbf{0}$, ($\beta$) $\mathbf{g}^{(0)}$ arising from the slip bound $g = 30$ in $(2.2)_6$. The former $\mathbf{g}^{(0)}$ results in the free-slip condition, i.e. $\boldsymbol{\sigma}_\tau = \mathbf{0}$ on S so the first iteration of MSA solves the linear problem. The characteristics of the method are summarized in Table 1. The columns $iter$, N_F denote the number of the fixed point iterations, and the number of the matrix–vector multiplications, respectively. The corresponding value for the initial approximation (α), (β) is given by the first integer, and the integer in parenthesis, respectively. The last column indicates the used value of the parameter ρ. The distribution of the tangential velocity $\boldsymbol{u}_\tau$ and the nonnegative function $\Psi = \mathscr{F}|\sigma_\nu| - \|\boldsymbol{\sigma}_\tau\|$ on S for different values of $\mathscr{F}$ is shown in Figs. 2, 3, 4. From Fig. 2 we see that for $\mathscr{F} = 0.03$ the fluid is slipping along the whole S. This is confirmed by the distribution of Ψ which is equal to zero practically everywhere in S. On the contrary, for (artificially) large $\mathscr{F} = 1100$ the fluid adheres to S and Ψ is positive in S. Finally, if $\mathscr{F} = 0.5$ then both stick and slip zones in S are present. It is worth noticing that the streamlines on S disappear (Fig. 3) meaning that the fluid leaves up S. In Figs. 5, 6 the evolution of the stick/slip zone during the iteration process is depicted. From there we see that if $\mathbf{g}^{(0)} = 0$, the process starts with the slip on the whole S unlike the pure stick on S for $\mathbf{g}^{(0)}$ from (β). Table 1 indicates that just a small number of the fixed point iterations is needed to get the solution with the

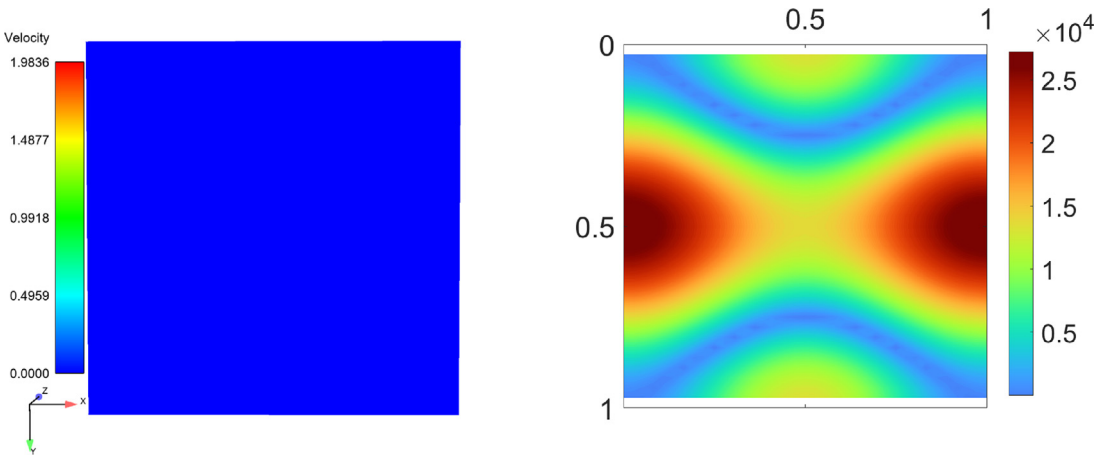

Fig. 4. Tangential velocity field (left), distribution of Ψ (right) on S; $\mathscr{F} = 1100$.

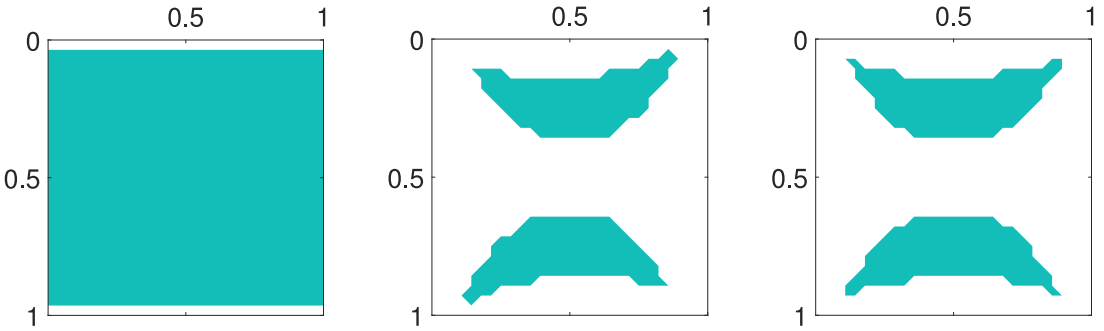

Fig. 5. Slip zones on S in MSA algorithm: 1. iter. (left), 2. iter. (center), 3. iter. (right); $\mathscr{F} = 0.5$, $\mathbf{g}^{(0)} = \mathbf{0}$.

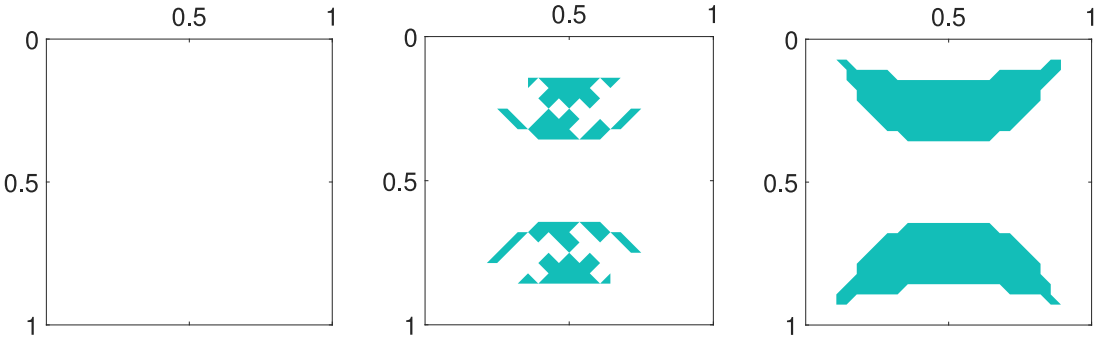

Fig. 6. Slip zones on S in MSA algorithm: 1. iter. (left), 2. iter. (center), 3. iter. (right); $\mathscr{F} = 0.5$, $\mathbf{g}^{(0)}$ from (β).

required precision. In addition, this number is practically the same for all finite element partitions. The low number of iterations for $\mathscr{F} = 1100$ and $\mathbf{g}^{(0)}$ from (β) is due to the fact that the first and the last iteration solve the Stokes system with the no-slip condition on the whole S, i.e. the linear problem.

The second experiment has been done with the SSN Coulomb algorithm. The physical data are the same as before. The parameters required by this algorithm are $\epsilon = 10^{-7}$, $\rho = 0.1$. The results are summarized in Table 2. The column $iter$ now denotes the number of the Newton steps and N_F has the same meaning as in Table 1. Unlike the MSA algorithm, in which the parameter ρ has to be carefully chosen to ensure positive definiteness of the block $\mathbf{A}_\rho$ in (5.7), the situation now is different since the system (5.16) is solved by the BCG type method. Comparing

Table 1
MSA with SSN Tresca solver; $\mathbf{g}^{(0)} = \mathbf{0}$, ($\mathbf{g}^{(0)}$ from β).

$n_u/n_p/n_c$	$\mathscr{F} = 0.03$		$\mathscr{F} = 0.5$		$\mathscr{F} = 1100$		ρ
	iter	N_F	*iter*	N_F	*iter*	N_F	
5148/2197/143	**3 (4)**	343 (614)	**6 (5)**	1359 (896)	**5 (2)**	833 (284)	10^{-3}
23 940/9261/399	**3 (4)**	498 (770)	**5 (5)**	1255 (1605)	**5 (2)**	1036 (257)	10^{-3}
65 772/24 389/783	**3 (4)**	492 (808)	**5 (5)**	1354 (1149)	**5 (2)**	1034 (356)	10^{-4}
139 860/50 653/1295	**3 (4)**	545 (872)	**5 (5)**	1422 (1322)	**5 (2)**	1199 (299)	10^{-4}
255 420/91 125/1935	**3 (4)**	530 (899)	**5 (5)**	1566 (1556)	**5 (2)**	1205 (350)	10^{-4}
421 668/148 877/2703	**3 (4)**	561 (979)	**5 (5)**	1669 (1657)	**5 (2)**	1270 (311)	10^{-4}

Table 2
Direct solution with SSN Coulomb solver; $\mathbf{g}^{(0)} = \mathbf{0}$, ($\mathbf{g}^{(0)}$ from β), $\rho = 0.1$.

$n_u/n_p/n_c$	$\mathscr{F} = 0.03$		$\mathscr{F} = 0.5$		$\mathscr{F} = 1100$	
	iter	N_F	*iter*	N_F	*iter*	N_F
5148/2197/143	**7 (6)**	138 (156)	**6 (6)**	147 (146)	**6 (4)**	70 (78)
23 940/9261/399	**7 (6)**	173 (194)	**7 (6)**	200 (178)	**4 (4)**	85 (94)
65 772/24 389/783	**7 (6)**	193 (226)	**7 (6)**	264 (274)	**6 (5)**	111 (125)
139 860/50 653/1295	**7 (6)**	223 (262)	**8 (7)**	311 (375)	**4 (4)**	121 (130)
255 420/91 125/1935	**7 (6)**	234 (351)	**7 (6)**	335 (357)	**4 (4)**	155 (183)
421 668/148 877/2703	**7 (6)**	270 (262)	**7 (8)**	345 (408)	**4 (4)**	114 (122)

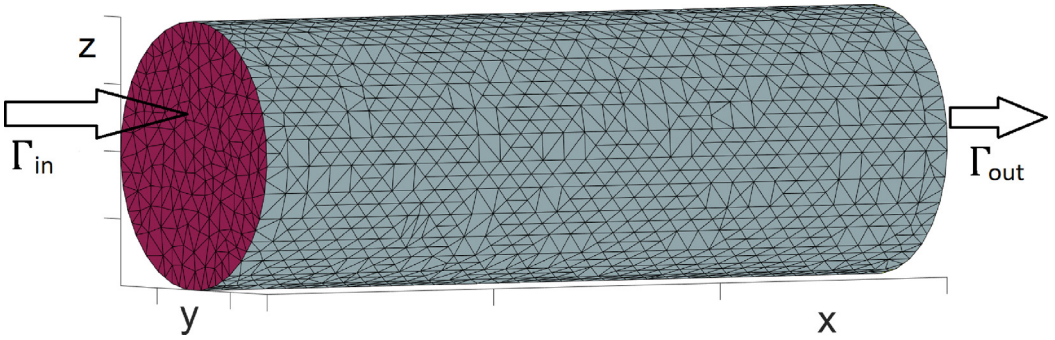

Fig. 7. Tube and 3D mesh.

the number of the fixed-point iterations *iter* in MSA (Table 1) with the number of the Newton steps *iter* (Table 2) we see that the latter is slightly higher. It turned out during computations that the Newton iterations have to be computed with higher accuracy compared with the MSA otherwise the Newton method may fail. Despite this fact, comparing the numbers N_F for MSA (Table 1) and SSN Coulomb solver (Table 2) we see that this number which can serve as one of possible indicators of efficiency of the used algorithms is considerably lower for the latter, in particular when stick–slip zones exist simultaneously. In addition, during numerical tests it emerged that SSN Coulomb algorithm is more robust as far as the choice of ρ is concerned in comparison with MSA. For this reason the next example will be solved by the SSN Coulomb solver.

Example 2 (*3D Tube*)**.** Let Ω be the tube of radius $r = 1$ and length $L = 6$ as in Fig. 7, where the finite element mesh $\mathscr{T}_h$ and the partition of the boundary $\partial\Omega = \overline{S} \cup \overline{\Gamma}_{in} \cup \overline{\Gamma}_{out}$ is depicted. On Γ_{in} we prescribe the input velocity $\mathbf{u} = (u_{max} - u_{max} \cdot (y^2 + z^2)/r^2, 0, 0)$, where $u_{max} = 0.5$ is the maximal velocity amplitude of the parabolic flow profile on Γ_{in}. The natural outflow condition $\boldsymbol{\sigma}_N = \mathbf{0}$ on Γ_{out} will be prescribed. Cylindrical surface of Ω represents the slip part S. Further $\mathbf{f} = \mathbf{0}$ in Ω, $\mu = 0.5$ and $\mathscr{F} \in \{0.001; 0.6; 0.7; 1000\}$. The smallest, largest value of $\mathscr{F}$ is again chosen to simulate the pure slip, and stick, respectively on S.

Table 3
Direct solution with SSN Coulomb solver.

$n_u/n_p/n_c$	$\mathscr{F} = 0.001$		$\mathscr{F} = 0.6$		$\mathscr{F} = 0.7$		$\mathscr{F} = 1000$	
	$iter$	N_F	$iter$	N_F	$iter$	N_F	$iter$	N_F
2292/813/410	**4**	700	**13**	4074	**9**	2784	**2**	436
4650 /1613/745	**4**	796	**18**	6722	**10**	3587	**2**	529
19 692/6751/1862	**4**	1059	**20**	7697	**11**	4264	**2**	752
38 169/13 000/3033	**4**	996	**25**	12 209	**14**	6690	**2**	685
61 611/20 920/4025	**4**	1054	**25**	12 775	**14**	6976	**2**	708

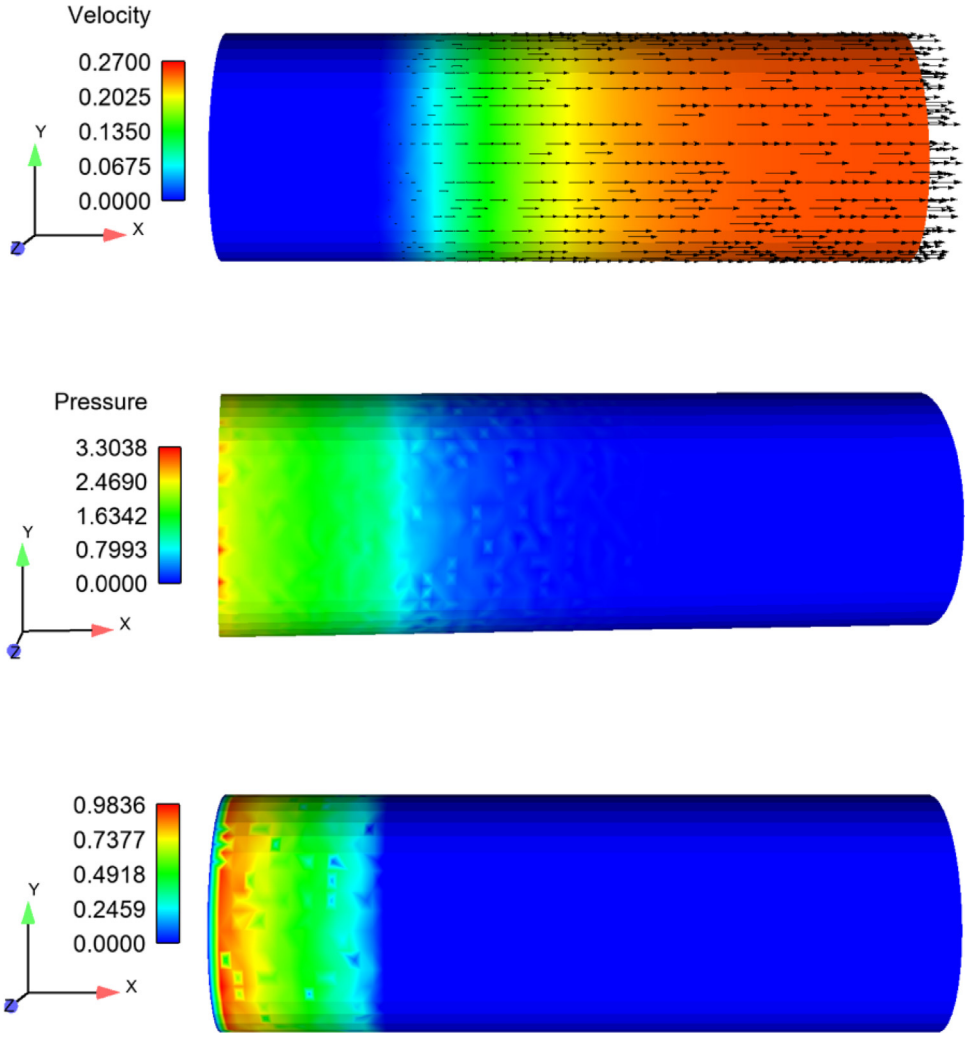

Fig. 8. Distribution of velocity (top), pressure (middle), the function Ψ (below) on S for $\mathscr{F} = 0.6$.

The results of the SSN Coulomb algorithm are summarized in Table 3. The low number of iterations for $\mathscr{F} = 0.0001$ and 1000 follows from the fact that the problems become linear. The parameters required by this algorithm are $\epsilon = 10^{-5}$, $\rho = 0.1$. The velocity, the pressure field and the distribution of the function Ψ on S in the simultaneous stick and slip case are seen from Figs. 8, 10 for $\mathscr{F} = 0.6$ and $\mathscr{F} = 0.7$, respectively using the numerical results on the finest mesh. Finally the velocity distribution on the selected cross sections of the tube are shown in Figs. 9 and 11.

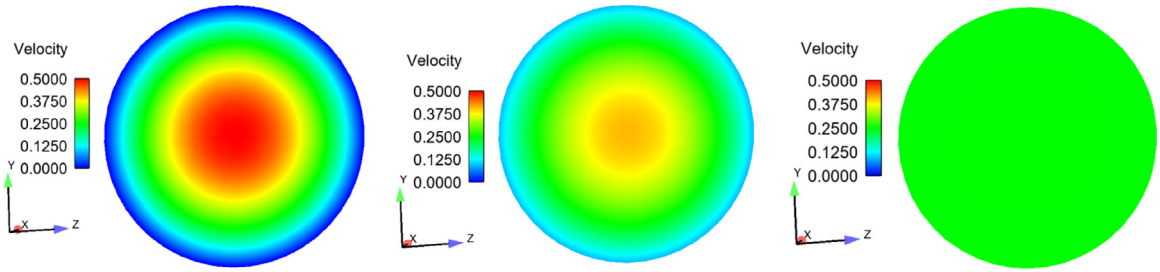

Fig. 9. Sectional view of the velocity distribution on Γ_{in} (left), on $x = 2$ (middle), on Γ_{out} (right) for $\mathscr{F} = 0.6$.

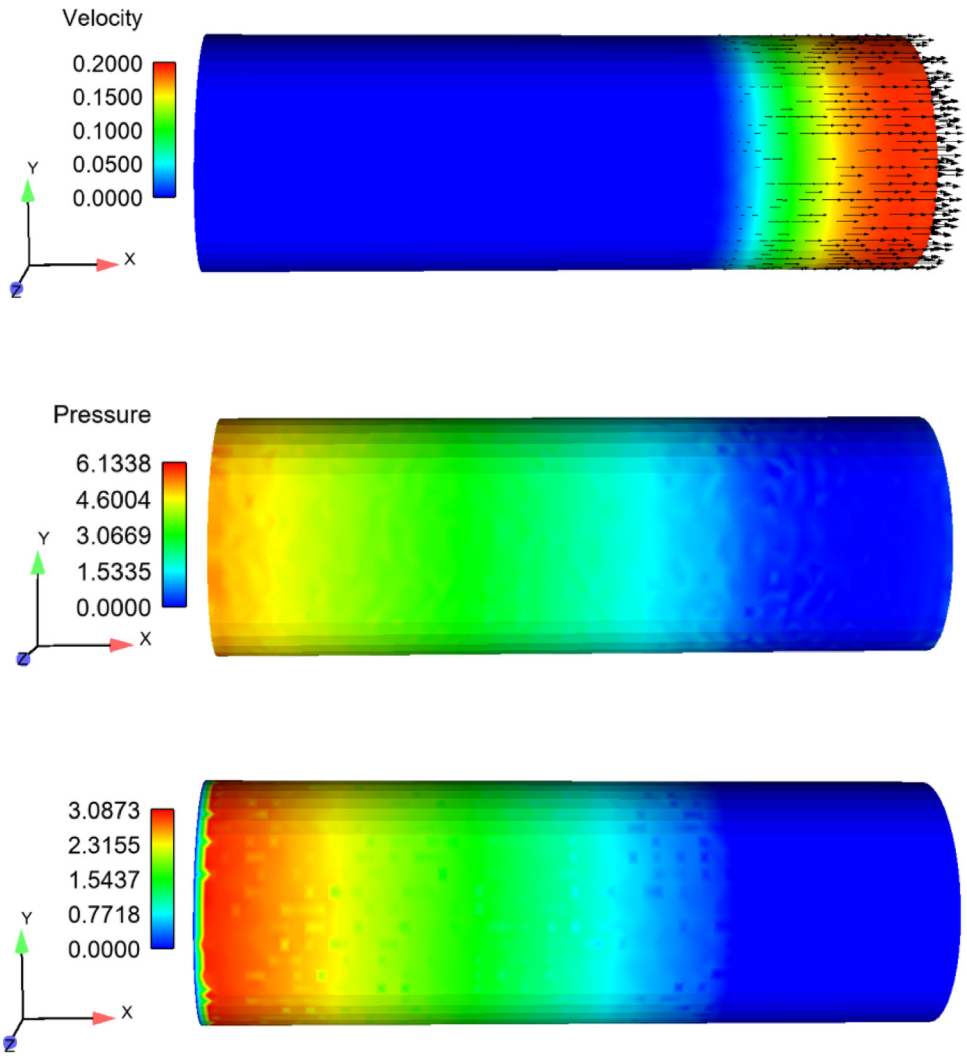

Fig. 10. Distribution of velocity (top), pressure (middle), the function Ψ (below) on S for $\mathscr{F} = 0.7$.

7. Conclusions

The theoretical part presents two weak settings of the problem in terms of the fluid velocity and pressure namely as (i) an implicit variational inequality and (ii) a fixed-point formulation. Since knowledge of the normal and shear stress on the slip part of the boundary is essential to numerical realization we also present the so-called four field

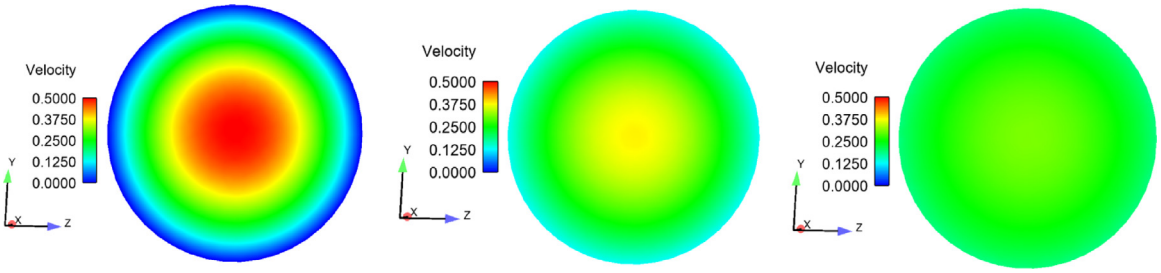

Fig. 11. Sectional view of the velocity distribution on $x = 3$ (left), on $x = 5$ (middle), on Γ_{out} (right) for $\mathscr{F} = 0.7$.

formulation in terms of the velocity, pressure, normal and shear stress as it enables us to compute all these quantities directly. Discretization of this formulation is done in an abstract way by the classical Galerkin type approach. Under appropriate assumptions on the used finite dimensional spaces we are able to guarantee the existence of at least solution to the discretized problems for any value of the discretization parameter h and of the slip coefficient $\mathscr{F}$. In addition, if $\mathscr{F}$ is sufficiently small, the discrete solution is unique. However, the condition ensuring uniqueness is mesh dependent. The second part of the paper is devoted to computational aspects. The discretized four field formulations lead to systems of non-smooth algebraic equations including projection mappings onto convex sets. Such systems are solved by a semi-smooth Newton type method using the active/inactive set implementation which is in details presented there. Finally, numerical experiments with two simple examples are presented and the above mentioned approaches (i) and (ii) are compared.

CRediT authorship contribution statement

Jaroslav Haslinger: Conceptualization, Methodology, Validation, Formal analysis, Investigation, Resources, Data curation, Supervision, Writing – original draft, Funding acquisition. **Radek Kučera:** Conceptualization, Methodology, Validation, Formal analysis, Investigation, Resources, Visualization, Supervision, Writing – review & Editing, Validation, Funding acquisition. **Kristina Motyčková:** Software, Validation, Visualization, Investigation, Project administration, Funding acquisition. **Václav Šátek:** Software, Validation, Visualization, Investigation, Funding acquisition.

Acknowledgments

This work was supported by the Ministry of Education, Youth and Sports of the Czech Republic through the e-INFRA CZ (ID:90140). The paper also includes the results of the internal BUT FIT project FIT-S-23-8151 (VS). J.H. acknowledges discussion with Yves Renard. The second author (RK) acknowledges the internal VSB-TUO project SGS-310. All authors have read and agreed to the published version of the manuscript.

References

[1] Iso2mesh: a 3D surface and volumetric mesh generator for MATLAB/octave, 2023, URL: http://iso2mesh.sourceforge.net. (online).
[2] Karolina - IT4innovations, 2023, URL: https://www.it4i.cz/en/infrastructure/karolina. (online).
[3] V. Arzt, Finite element meshes and assembling of stiffness matrices (Masters thesis), VŠB-TU Ostrava, Czech Republic, 2019, in czech.
[4] M. Ayadi, H. Ayed, L. Baffico, T. Sassi, Stokes problem with slip boundary conditions of friction type: Error analysis of a four-field mixed variational formulation, J. Sci. Comput. 81 (5) (2019) 312–341.
[5] M. Ayadi, L. Baffico, M.K. Gdoura, T. Sassi, Error estimates for Stokes problem with Tresca friction conditions, ESAIM: M2AN 48 (2014) 1413–1429.
[6] M. Boukrouche, L. Paoli, Global existence for a 3D non-stationary Stokes flow with Coulomb's type friction boundary conditions, Appl. Anal. 97 (8) (2018) 1385–1415.
[7] J.H. Bramble, J.E. Pasciak, O. Steinbach, On the stability of the L^2 projection in $H^1(\Omega)$, Math. Comp. 71 (237) (2001) 147–156.
[8] F. Brezzi, M. Fortin, Mixed and Hybrid Finite Element Methods, Springer Series in Computational Mathematics, Springer Verlag, 1991.
[9] P.G. Ciarlet, The finite element method for elliptic problems, North-Holland, Amsterdam, New York, Oxford, 1978.
[10] L. Consiglieri, A non-local friction problem for a class of non-Newtonian flows, Porth. Math. 60 (2003) 237–252.

[11] J.K. Djoko, J. Koko, Numerical methods for the Stokes and Navier-Stokes equations driven by slip boundary conditions, Comput. Methods Appl. Mech. Engrg. 305 (2016) 936–958.
[12] J.K. Djoko, M. Mbehou, Finite element analysis for Stokes and Navier Stokes equations driven by threshold slip boundary conditions, Int. J. Numer. Anal. Model. Ser. B4 (2013) 235–255.
[13] H.C. Elman, D.J. Silvester, A.J. Wathen, Finite Elements and Fast Iterative Solvers: With Applications in Incompressible Fluid Dynamics, Numerical Mathematics and Scientific Computation, Oxford University Press, 2014.
[14] F. Facchinei, F. Pang, Finite-Dimensional Variational Inequalities and Complementarity Problems, Vol. I and II, Springer, New York, 2003.
[15] H. Fujita, A mathematical analysis of motions of viscous incompressible fluid under leak and slip boundary conditions, RIMS Kokyuroku 888 (1994) 199–216.
[16] H. Fujita, A coherent analysis of Stokes flows under boundary conditions of friction type, J. Comput. Appl. Math. 149 (2002) 57–69.
[17] V. Girault, P.A. Raviart, Finite Element Methods for Navier-STokes Equations, Springer Series in Computational Mathematics, Springer Verlag, 1986.
[18] R. Glowinski, Numerical methods for nonlinear variational problems, Springer Series in Computational Physics, Springer Verlag, 1983.
[19] J. Haslinger, R. Kučera, T. Sassi, V. Šátek, Dual strategies for solving the Stokes problem with stick-slip boundary conditions in 3D, Math. Comput. Simulation 189 (2021) 191–206.
[20] J. Haslinger, R. Kučera, V. Šátek, The semi-smooth Newton method for solving the Stokes flow with Coulomb slip boundary conditions, AIP Conf. Proc. 2116 (2019).
[21] J. Haslinger, R. Kučera, V. Šátek, Stokes system with local Coulomb's slip boundary conditions: Analysis of discretized models and implementation, Comput. Math. Appl. 77 (2019) 1655–1667.
[22] J. Haslinger, R. Kučera, V. Šátek, T. Sassi, Stokes system with solution-dependent threshold slip boundary conditions: Analysis, approximation and implementation, Math. Mech. Solids 23 (3) (2018) 294–307.
[23] J. Haslinger, J. Stebel, Stokes problem with a solution dependent slip bound: Stability of solutions with respect to domains, ZAMM - J. Appl. Math. Mech. 96 (9) (2016) 1049–1060.
[24] M. Hintermüller, K. Ito, K. Kunisch, The primal-dual active set strategy as a semismooth Newton method, SIAM J. Optim. 13 (3) (2002) 865–888.
[25] T. Kashiwabara, On a finite element approximation of the Stokes equations under a slip boundary condition of the friction type, Japan J. Industr. Appl. Math. 30 (2013) 227–261.
[26] J. Koko, Efficient MATLAB codes for the 2D/3D Stokes equation with the mini-element, Informatica 30 (2) (2019) 243–268.
[27] R. Kučera, V. Arzt, J. Koko, Free available vectorized codes, 2023, URL: https://homel.vsb.cz/~kuc14/programs/ReferenceAssembling.zip. (online).
[28] R. Kučera, J. Machalová, H. Netuka, P. Ženčák, An interior point algorithm for the minimization arising from 3D contact problems with friction, Optim. Methods Softw. 28 (6) (2013) 1195–1217.
[29] R. Kučera, K. Motyčková, A. Markopoulos, J. Haslinger, On the inexact symmetrized globally convergent semi-smooth Newton method for 3D contact problems with tresca friction: the R-linear convergence rate, Optim. Methods Softw. 35 (1) (2020) 65–86.
[30] J. Nečas, Direct Methods in Theory of Elliptic Equations, Springer Monographs in Mathematics, Springer Heidelberg, Dordrecht, London, New York, 2012.
[31] J. Rao, K. Rajagopal, The effect of the slip boundary conditions on the flow of fluids in a channel, Acta Mech. 135 (1999) 113–126.
[32] C. le Roux, Steady Stokes flows with threshold slip boundary conditions, Math. Models Meth. Appl. Sci. 15 (2005) 1141–1168.
[33] C. le Roux, A. Tani, Steady solutions of the Navier-Stokes equations with threshold slip boundary conditions, Math. Methods Appl. Sci. 30 (2007) 595–624.
[34] N. Saito, On the Stokes equation with the leak and slip boundary conditions of friction type: Regularity of solutions, Publ. RIMS, Kyoto Univ. 40 (2004) 345–383.